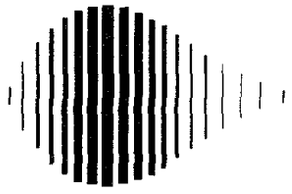

NATIONAL CENTER FOR EARTHQUAKE ENGINEERING RESEARCH

State University of New York at Buffalo

AN EXPERIMENTAL STUDY OF SEISMIC STRUCTURAL RESPONSE WITH ADDED VISCOELASTIC DAMPERS

by

R.C. Lin, Z. Liang, T.T. Soong and R.H. Zhang

Department of Civil Engineering
State University of New York at Buffalo
Buffalo, NY 14260

REPRODUCED BY
U.S. DEPARTMENT OF COMMERCE
NATIONAL TECHNICAL INFORMATION SERVICE
SPRINGFIELD, VA. 22161

Technical Report NCEER-88-0018

June 30, 1988

This research was conducted at the State University of New York at Buffalo and was partially supported by the National Science Foundation under Grant No. ECE 86-07591.

NOTICE

This report was prepared by the State University of New York at Buffalo as a result of research sponsored by the National Center for Earthquake Engineering Research (NCEER) and the National Science Foundation. Neither NCEER, associates of NCEER, its sponsors, State University of New York at Buffalo, nor any person acting on their behalf:

a. makes any warranty, express or implied, with respect to the use of any information, apparatus, method, or process disclosed in this report or that such use may not infringe upon privately owned rights; or

b. assumes any liabilities of whatsoever kind with respect to the use of, or for damages resulting from the use of, any information, apparatus, method or process disclosed in this report.

PB89-122212

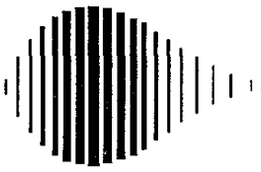

AN EXPERIMENTAL STUDY OF SEISMIC STRUCTURAL RESPONSE WITH ADDED VISCOELASTIC DAMPERS

by

R.C. Lin[1], Z. Liang[2], T.T. Soong[3] and R.H. Zhang[4]

June 30, 1988

Technical Report NCEER-88-0018

NCEER Contract Number 86-3025

Master Contract Number ECE 86-07591

1 Research Associate, Dept. of Civil Engineering, State University of New York at Buffalo
2 Research Associate, Dept. of Civil Engineering, State University of New York at Buffalo
3 Professor, Dept. of Civil Engineering, State University of New York at Buffalo
4 Visiting Scholar, Dept. of Civil Engineering, State University of New York at Buffalo

NATIONAL CENTER FOR EARTHQUAKE ENGINEERING RESEARCH
State University of New York at Buffalo
Red Jacket Quadrangle, Buffalo, NY 14261

REPRODUCED BY
U.S. DEPARTMENT OF COMMERCE
NATIONAL TECHNICAL
INFORMATION SERVICE
SPRINGFIELD, VA 22161

50272-101

REPORT DOCUMENTATION PAGE	1. REPORT NO. NCEER-88-0018	2.	3. Recipient's Accession No. PB89-122212/AS

4. Title and Subtitle
An Experimental Study of Seismic Structural Response with Added Viscoelastic Dampers

5. Report Date
June 30, 1988

6.

7. Author(s)
R.C. Lin, Z. Liang, T.T. Soong and R. H. Zhang

8. Performing Organization Rept. No.

9. Performing Organization Name and Address
National Center for Earthquake Engineering Research
State University of New York at Buffalo
Red Jacket Quadrangle
Buffalo, NY 14261

10. Project/Task/Work Unit No.

11. Contract(C) or Grant(G) No.
(C) ECE 86-07591
(G)

12. Sponsoring Organization Name and Address

13. Type of Report & Period Covered
Technical Report

14.

15. Supplementary Notes
This research was conducted at the State University of New York at Buffalo and was partially supported by the National Science Foundation under Grant No.ECE-86-07591.

16. Abstract (Limit: 200 words)

The feasibility of using viscoelastic dampers to mitigate earthquake-induced structural response is studied experimentally. Two series of experiments were conducted using a model structure simulating a single-degree-of-freedom structure and a three-degree-of-freedom structure. Reductions in relative displacements and absolute accelerations are used as the measure of effectiveness of added viscoelastic dampers. Temperature dependency of the dampers is carefully examined together with the problem of damper placement.

Experimental as well as simulation results show that significant improvement of structural performance under seismic conditions can be realized with addition of viscoelastic dampers. It is shown that the damper effectiveness is strongly dependent upon the environmental temperature. The importance of their placements within the structure is also stressed.

17. Document Analysis a. Descriptors

b. Identifiers/Open-Ended Terms
VISCOELASTIC DAMPERS
EARTHQUAKE ENGINEERING
STRUCTURAL RESPONSE
SEISMIC EXCITATION

c. COSATI Field/Group

18. Availability Statement	19. Security Class (This Report)	21. No. of Pages
Release unlimited	unclassified	78
	20. Security Class (This Page) unclassifed	22. Price A05

(See ANSI-Z39.18) See Instructions on Reverse OPTIONAL FORM 272 (4-77) (Formerly NTIS-35)

PREFACE

The National Center for Earthquake Engineering Research (NCEER) is devoted to the expansion of knowledge about earthquakes, the improvement of earthquake-resistant design, and the implementation of seismic hazard mitigation procedures to minimize loss of lives and property. Initially, the emphasis is on structures and lifelines of the types that would be found in zones of moderate seismicity, such as the eastern and central United States.

NCEER's research is being carried out in an integrated and coordinated manner following a structured program. The current research program comprises four main areas:

- Existing and New Structures
- Secondary and Protective Systems
- Lifeline Systems
- Disaster Research and Planning

This technical report pertains to Program 2, Secondary and Protective Systems, and more specifically, to a passive protective system. Protective Systems are devices or systems which, when incorporated into a structure, help to improve the structure's ability to withstand seismic or other environmental loads. These systems can be passive, such as base isolators or viscoelastic dampers; or active, such as active tendons or active mass dampers; or combined passive-active systems.

Passive protective systems constitute one of the important areas of research. Current research activities, as shown schematically in the figure below, include the following:

1. Compilation and evaluation of available data.
2. Development of comprehensive analytical models.
3. Development of performance criteria and standardized testing procedures.
4. Development of simplified, code-type methods for analysis and design.

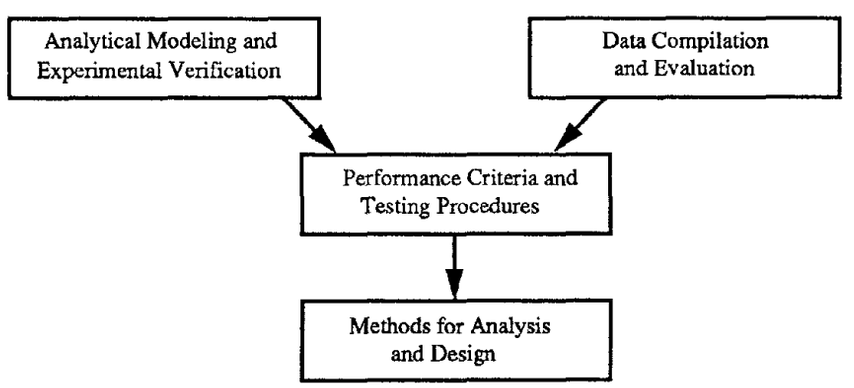

The Center provided partial funding to the State University of New York at Buffalo and the University of California at Berkeley to conduct comprehensive experimental research on the possible use of viscoelastic dampers as a passive protective system for building structures. This report presents the results of experimental research carried out at SUNY/Buffalo. The following sections detail the experiments performed, results obtained, and conclusions that can be drawn from this experimental investigation.

ABSTRACT

The feasibility of using viscoelastic dampers to mitigate earthquake-induced structural response is studied experimentally. Two series of experiments were conducted using a model structure simulating a single-degree-of-freedom structure and a three-degree-of-freedom structure. Reductions in relative displacements and absolute accelerations are used as the measure of effectiveness of added viscoelastic dampers. Temperature dependency of the dampers is carefully examined together with the problem of damper placement.

Experimental as well as simulation results show that significant improvement of structural performance under seismic conditions can be realized with addition of viscoelastic dampers. It is shown that the damper effectiveness is strongly dependent upon the environmental temperature. The importance of their placements within the structure is also stressed.

ACKNOWLEDGEMENTS

The authors are grateful to Dr. P. Mahmoodi, Corporate Scientist of the 3M Company, for his interest and technical contributions to this research program. The viscoelastic dampers used in these experiments were contributed by the 3M Company. Student support provided by the 3M Company is also gratefully acknowledged.

Thanks are also due Messrs. Mark Pitman and Dan Walch, who are responsible for operating the Earthquake Simulator Facility at the State University of New York at Buffalo.

This research was supported in part by the National Center for Earthquake Engineering Research, State University of New York at Buffalo, under Grant No. NCEER-86-3025.

Preceding page blank

TABLE OF CONTENTS

SECTION	TITLE	PAGE
1	**INTRODUCTION**	1-1
2	**PROPERTIES OF VISCOELASTIC DAMPERS**	2-1
2.1	Background	2-1
2.2	Experimental Set-up and Program	2-1
2.3	Experimental Results	2-3
2.4	Analysis of the Experimental Results	2-11
3	**SINGLE-DEGREE-OF-FREEDOM SYSTEM**	3-1
3.1	Introduction	3-1
3.2	Basic Equations	3-1
3.3	Equivalent Stiffness and Damping Ratio	3-3
3.4	Experimental Set-up and Results	3-5
4	**MULTIPLE-DEGREE-OF-FREEDOM SYSTEM**	4-1
4.1	Experimental Set-up	4-1
4.2	Experimental Results and Discussion	4-1
5	**CONCLUDING REMARKS**	5-1
6	**REFERENCES**	6-1

Preceding page blank

LIST OF ILLUSTRATIONS

FIGURE	TITLE	PAGE
2.1	Typical Damper Structure	2-2
2.2	Experimental Set-up	2-4
2.3	Displacement-Force Time Histories and Hysteresis Loops at Different Temperatures (Frequency = 0.5 HZ)	2-6
2.4	Displacement-Force Time Histories and Hysteresis Loops at Different Frequencies (Temperature = 27.9°C)	2-8
2.5	Variations of G" with (a) Temperature and (b) Frequency	2-15
3.1	Input and Output Spectral Density Functions	3-2
3.2	Sample Function of a Narrow-band Process	3-4
3.3	Possible Damper Configurations	3-6
3.4	Experimental Set-up for SDOF System	3-8
3.5	Seismic Input for SDOF System	3-9
3.6	Damper Effect on Relative Displacement	3-12
3.7	Damper Effect on Absolute Acceleration	3-13
3.8	Absolute Acceleration Frequency Transfer Function	3-14
3.9	Temperature Dependence of Damping Factor	3-15
3.10	Temperature Dependence of Natural Frequency	3-16
3.11	Comparison of Experimental and Simulation Results in Maximum Relative Displacement	3-17
3.12	Comparison of Experimental and Simulation Results in Maximum Absolute Acceleration	3-18
4.1	Experimental Set-up - MDOF System	4-2
4.2	First-floor Relative Displacement for Case 1	4-3
4.3	Second-floor Relative Displacement for Case 1	4-4
4.4	Third-floor Relative Displacement for Case 1	4-5
4.5	First-floor Absolute Acceleration Frequency Transfer Function for Case 1	4-6
4.6	Second-floor Absolute Acceleration Frequency Transfer Function for Case 1	4-7
4.7	Third-floor Absolute Acceleration Frequency Transfer Function for Case 1	4-8
4.8	First-floor Relative Displacement (No Damper)	4-10
4.9	Second-floor Relative Displacement (No Damper)	4-11
4.10	Third-floor Relative Displacement (No Damper)	4-12
4.11	First-floor Relative Displacement for Case 1 (T = 22.2°C)	4-13
4.12	Second-floor Relative Displacement for Case 1 (T = 22.2°C)	4-14
4.13	Third-floor Relative Displacement for Case 1 (T = 22.2°C)	4-15

Preceding page blank

LIST OF ILLUSTRATIONS (Cont'd)

FIGURE	TITLE	PAGE
5.1	Maximum Relative Displacement as a Function of Damping Ratio	5-3
5.2	Maximum Absolute Acceleration as a Function of Damping Ratio	5-4

LIST OF TABLES

TABLE	TITLE	PAGE
2.1	Damper Dimensions and Maximum Displacements	2-5
2.2	G′ and G" for Damper No. 1 at Different Temperatures and Frequencies	2-12
2.3a	G′ and G" of Damper Nos. 2, 3 and 4 at Different Temperatures	2-13
2.3b	G′ and G" of Damper Nos. 5, 6 and 7 at Different Temperatures	2-14
3.1	Experimental Results - SDOF System and Seismic Input	3-10
3.2	Results for Different Damper Configurations	3-20
4.1	Experimental Results - MDOF System and Seismic Input	4-17
4.2	System Parameters Based on Experimental Results	4-18
4.3	Simulation Results	4-19

SECTION 1

INTRODUCTION

Strong earthquake ground motion can cause excessive structural deformation and damage. Many means of enhancing structural seismic performance have been studied. These include passive energy absorbing devices such as base isolation, and active structural control through which structural dynamic characteristics can be modified.

The focus of this study is on the possible use of viscoelastic dampers as energy absorbing devices and on the question of whether they can be effective in reducing structural response to seismic excitations when installed in a building structure. It has been shown that wind-induced sway of high rise buildings can be significantly reduced by adding viscoelastic dampers to the structures [1-4], examples of which are the World Trade Center in New York City and the Columbia Center in Seattle.

The feasibility of using viscoelastic dampers to mitigate earthquake-induced structural response was studied recently [5]. Using computer simulation, the results show that the damped response of tall frame structures can be significantly reduced. The primary purpose of this investigation is to carry out an experimental investigation using a scaled-down model structure in the laboratory.

The model structure is a steel frame modeling a shear building by the method of artificial mass simulation [6]. It is similar in geometry, material properties and boundary conditions to a structural model extensively tested at other institutions and it is approximately a 1:4 scaled model of a prototype structure (1:2 scaled model), which has also been extensively tested under seismic conditions. In the first test series, the model is rigidly braced on the top two floors to simulate a

single-degree-of-freedom system and, in the second, the braces are removed so that the dynamic behavior of a multi-degree-of-freedom structure can be studied.

The base motion of the model structure is supplied by the SUNY/Buffalo shaking table. This table has five degrees of freedom, of which three (vertical, lateral and roll) can be individually programmed. The other two are controlled only for correction, and the sixth is constrained by two hydrostatic bearings. Input signals to the table can be of the following types: harmonic motions (sinusoidal, square, triangular), random motions, and any recorded earthquake motion from the PDP-11/13 library of 3000 recorded accelerograms.

A total of 18 viscoelastic dampers were selected for this study and they were supplied by the 3M Company. The dynamic characteristics of these dampers are first determined in the laboratory as reported in Section 2. Sections 3-5 detail the experiments performed, results obtained and conclusions that can be drawn from this experimental investigation.

SECTION 2

PROPERTIES OF VISCOELASTIC DAMPERS

2.1 BACKGROUND

Viscoelastic materials have made possible the recent development of an energy dissipation device called the viscoelastic (VE) damper. Incorporation of this device into a structure can improve the structure's dynamic performance by absorbing a substantial amount of vibrational energy. The mechanical properties of viscoelastic materials are rather complicated and may vary with environmental temperature and excitation frequency. Thus to properly interpret and understand the results from a structural test, it is necessary to know the properties of the dampers that are used in the test. Some experiments should therefore be carried out to determine the characteristics of specific dampers.

Reported below are the procedure and results of an extensive test that measured the response of eight VE dampers to variations in temperature and the response of one of those dampers to variations in excitation frequency. These tested dampers were later used in the structural tests.

2.2 EXPERIMENTAL SET-UP AND PROGRAM

Viscoelastic dampers can be classified into several categories based on the way in which the VE material layer deforms. For example, extension type dampers have VE layers that undergo extension and compression while shear type dampers have VE layers that experience nearly pure shear. The shear type dampers were used in this test. Figure 2.1 shows a shear VE damper consisting of two VE layers bounded between three steel plates. When the central steel plate moves relative to the outer two, the VE layers deform in shear.

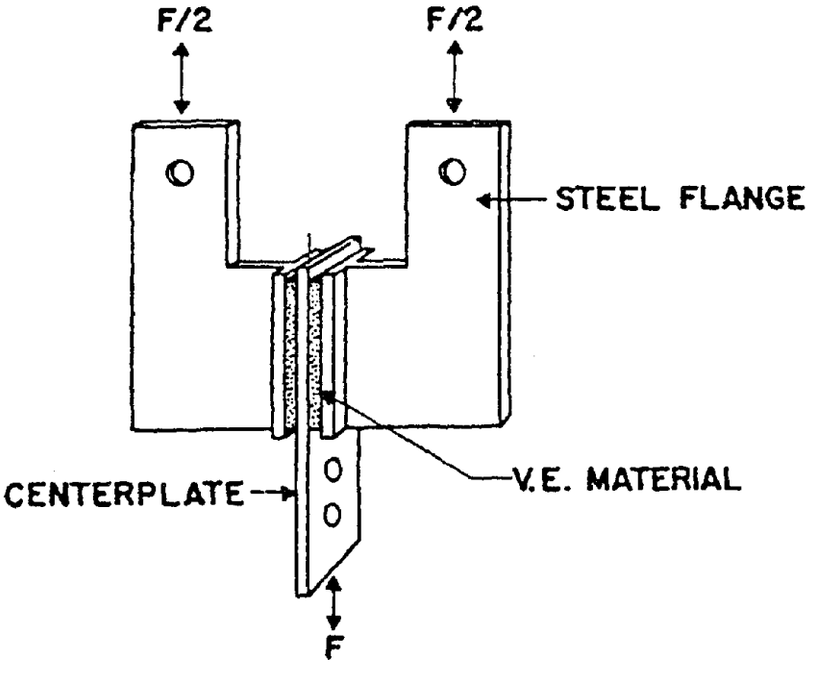

FIG. 2.1. Typical Damper Structure

The dampers were properly mounted to an MTS hydraulic actuator with connectors. The actuators were controlled by an MTS 406 Controller and an MTS 436 Control Unit which jointly controlled the amplitude, frequency, and loading cycle number. The control unit can be programmed to generate sine waves, triangular waves, etc.; however, only sinusoidal waves were used in this test. The amplitude of the motion was controlled to produce 40% and 50% strains on dampers of different thicknesses. During the test, damper displacement was monitored by an internal LVDT mounted at the end of the actuator. The force applied to the damper was measured via a load cell placed between the actuator loading rod and the damper. The measured signals were then sent to a SD380 Signal Analyzer which gave an accurate reading of the values over a time history display. The SD380 signal Analyzer can also give an "displacement vs force" plot which forms a hysteretic loop of the damper indicating the amount of energy dissipated in each deformation cycle. Figure 2.2 is a picture showing part of the experimental set-up, including the actuator, load cell, damper, etc.

Each damper was tested under three to five different temperatures to see the extent to which the damper's properties are dependent on temperature. One of the dampers was also loaded under four different frequencies to investigate the effect of frequency on the damper's characteristics.

2.3 EXPERIMENTAL RESULTS

A total of eight dampers consisting of three different dimensions were tested. Table 2.1 gives the area and thickness of each of the dampers.

The time history and hysteretic plots of damper #1 under five different temperatures and four different frequencies are given in Figs. 2.3 and 2.4, respectively. The maximum displacement of each of the dampers

Reproduced from
best available copy.

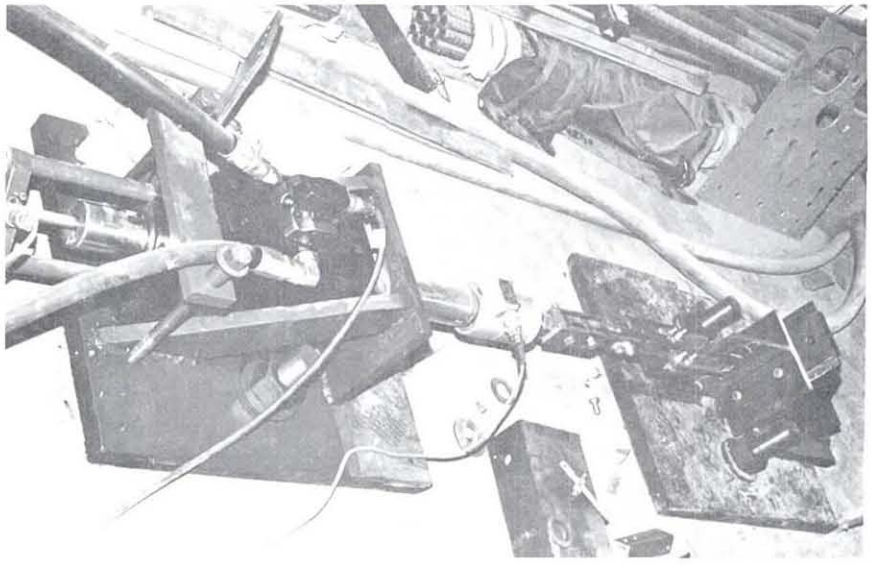

FIG. 2.2. Experimental Set-up

Damper No.	1	2	3	4	5	6	7	8
Area (in^2)	2.0	2.0	2.0	2.0	5.0	5.0	2.0	2.0
Thick. (in)	0.24	0.24	0.1	0.1	0.1	0.1	0.1	0.1
Max. Displ.(in)	0.1	0.1	0.05	0.05	0.05	0.05	0.05	0.05

TABLE 2.1. Damper Dimensions and Maximum Displacements

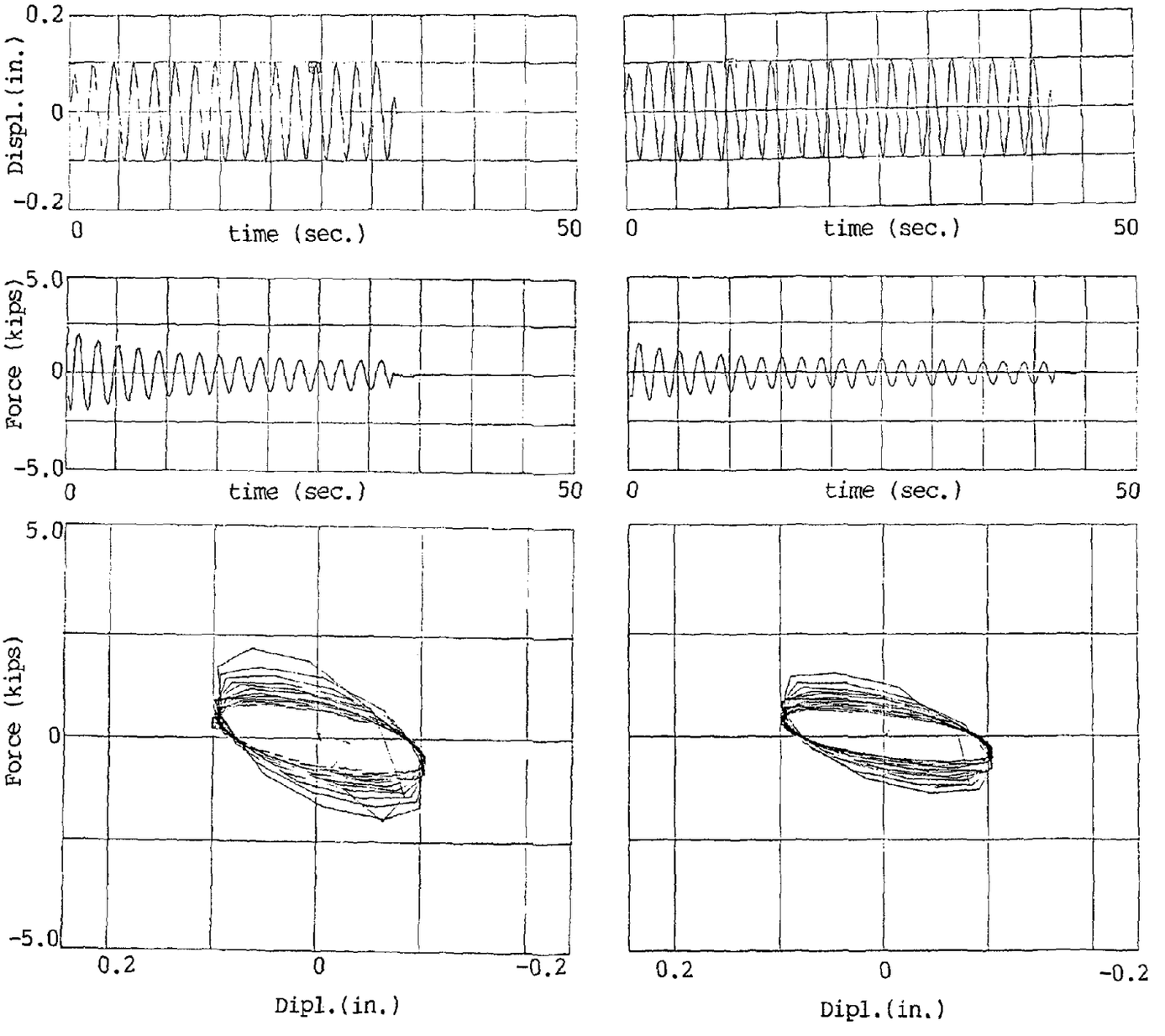

(i) T = 22.9°C

(ii) T = 25.5°C

FIG. 2.3a. Displacement-Force Time Histories and Hysteresis Loops at Different Temperatures (Frequency = 0.5 HZ)

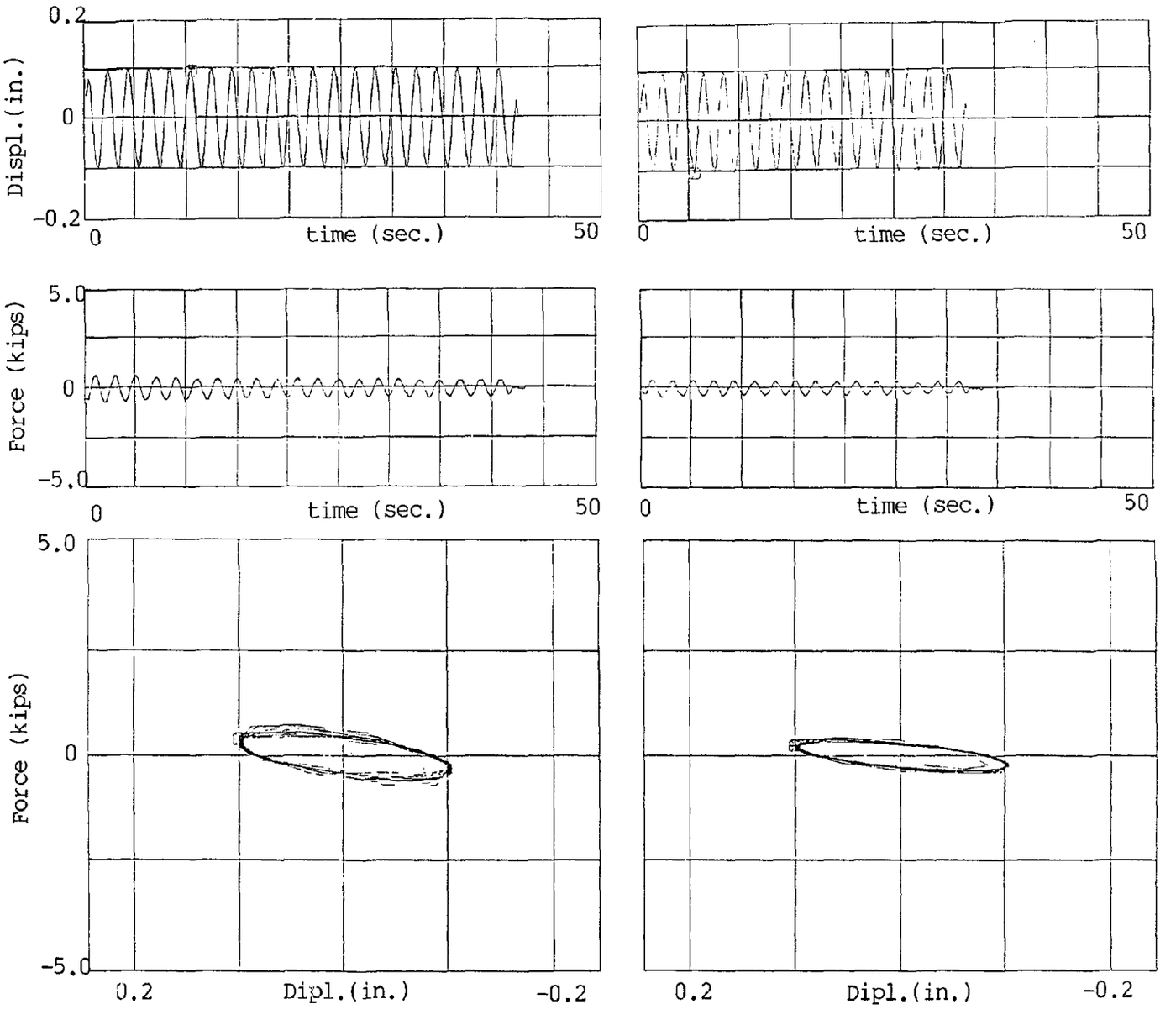

(iii) T = 31.4°C

(iv) T = 33.1°C

FIG 2.3b. Displacement-Force Time Histories and Hystresis Loops at Different Temperatures (Frequency = 0.5 HZ)

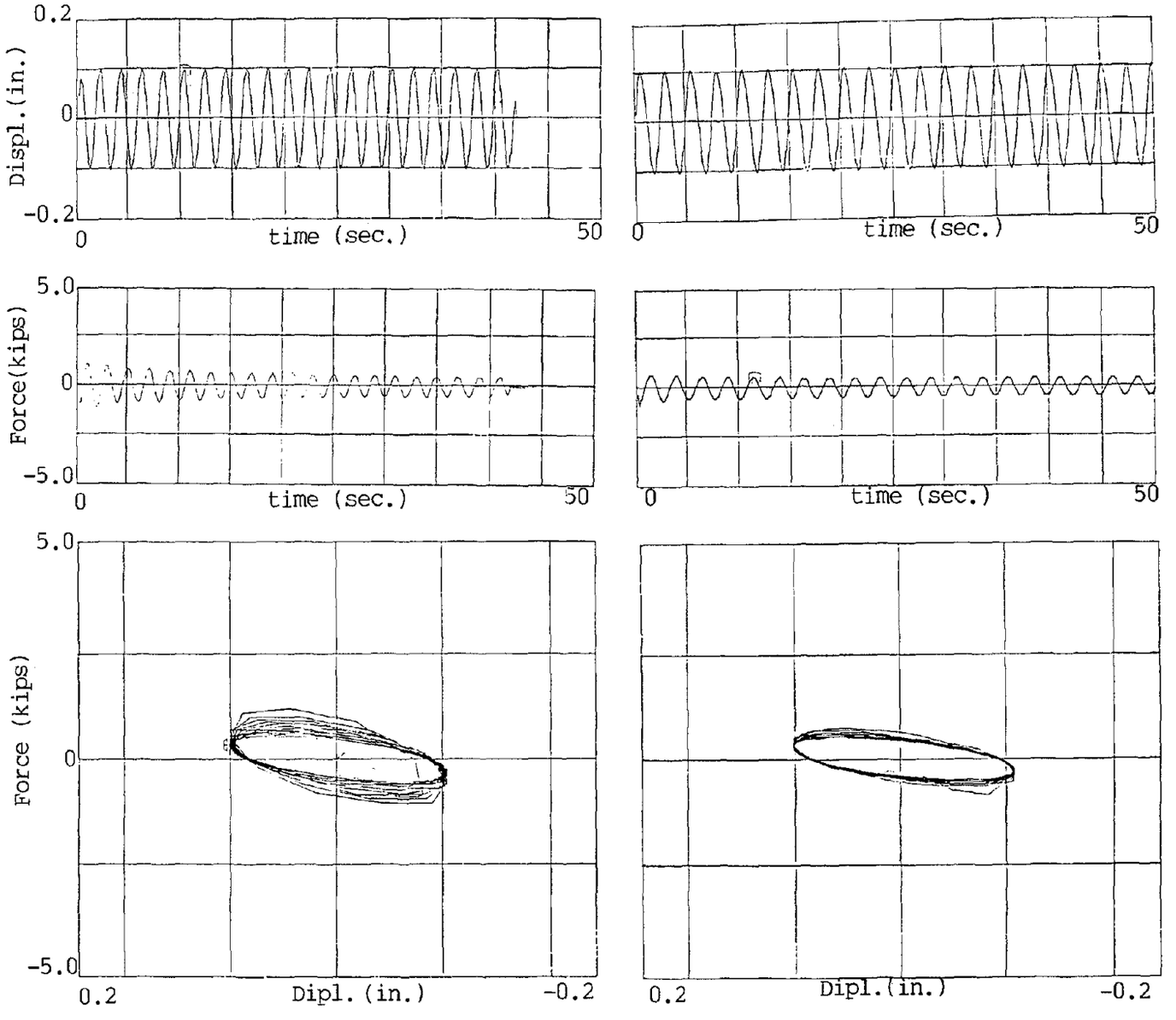

(i) f = 0.5 HZ

(ii) f = 0.2 HZ

FIG. 2.4a. Displacement-Force Time Histories and Hysteresis Loops at Different Frequencies (Temperature = 27.9°C)

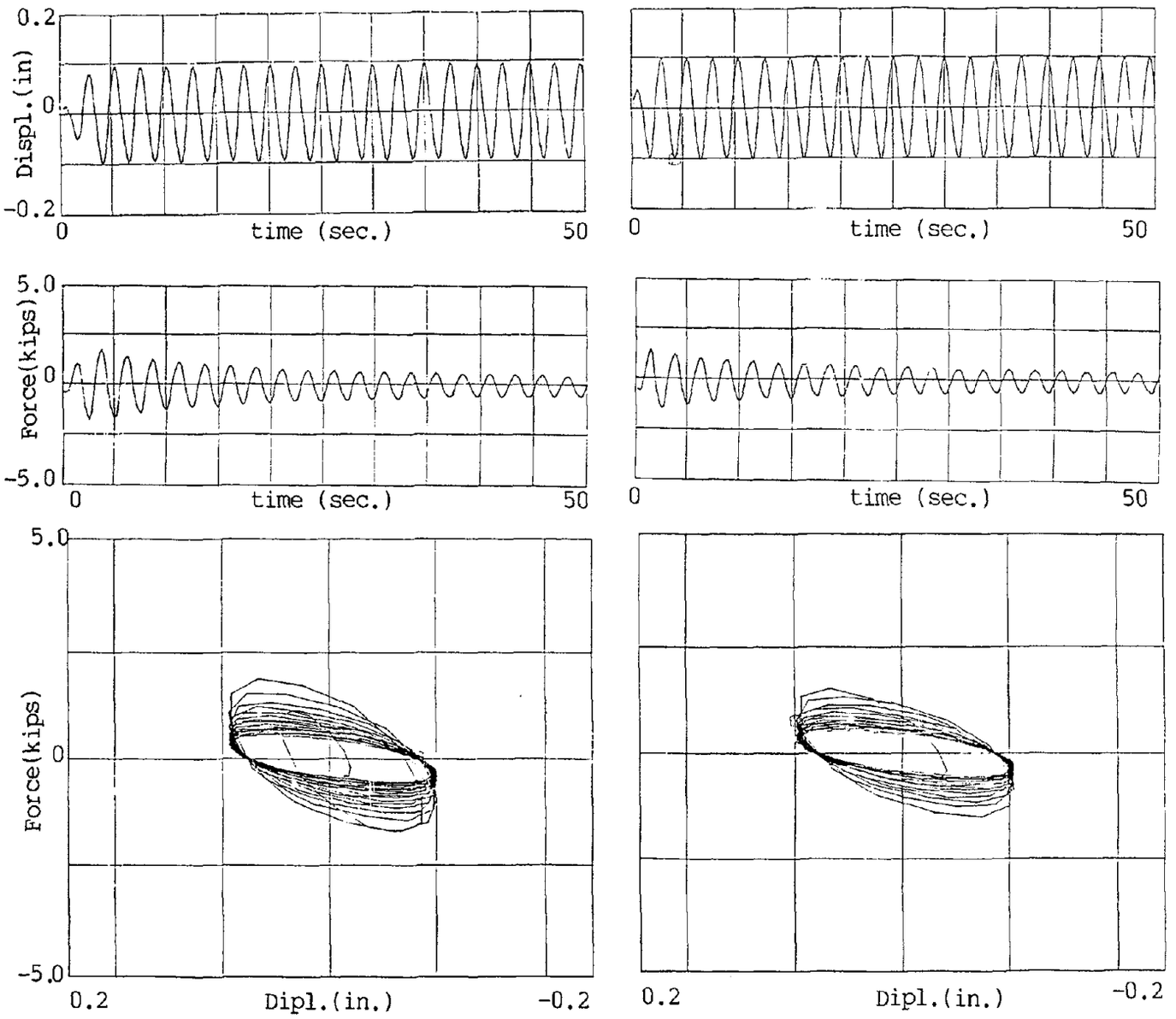

(iii) f = 2.0 HZ

(iv) f = 1.0 HZ

FIG. 2.4b. Displacement-Force Time Histories and Hystresis Loops at Different Frequencies (Temperature = 27.9^{o}C)

tested are listed in Table 2.1. From Fig. 2.3 it is evident that, if the maximum displacement value is kept constant, the change in maximum force during each cycle follows a pattern of damped-free oscillation. This pattern differs from damped-free vibration in that its maximum force approaches a constant value after a certain number of cycles.

According to the linear theory of viscoelasticity, the stress in a VE material under sinusoidal loading is proportional to the strain and the leading phase angle δ. Thus, if strain has the form

$$\gamma = \gamma_o \sin\omega t \tag{2.1}$$

the stress can be calculated from

$$\sigma = \sigma_o \sin(\omega t+\delta) \tag{2.2}$$

The relationship between stress and strain can be expressed as

$$\sigma = G^* \gamma_o \sin(\omega t+\delta) = \gamma_o (G' \sin\omega t + G'' \cos\omega t) \tag{2.3}$$

where

$$G^* = (G'^2 + G''^2)^{1/2} \tag{2.4}$$

is the module of the complex shear modulus. The quantity

$$G' = G^* \cos\delta \tag{2.5}$$

is called the shear storage modulus, and

$$G'' = G^* \sin\delta \tag{2.6}$$

is called the shear loss modulus.

Let the applied force be

$$F = F_o \sin\omega t \tag{2.7}$$

The relationship among the amplitudes of force, stress and strain are

$$F_o = \sigma_o A = \gamma_o G^* A \tag{2.8}$$

The damper's displacement is

$$\Delta_o = \gamma_o t$$

In the above, A and t are, respectively, damper area and thickness.

Since

$$F_o = k\gamma_o t$$

one has

$$\gamma_o G^* A = k\gamma_o t$$

and therefore

$$G^* = kt/A \tag{2.9}$$

The stiffness k can be calculated by dividing force magnitude F_o by the maximum displacement.

The time histories of the displacement and force in each of the dampers were measured and recorded. They were then used to find damper stiffness and the phase angle. Using the above equations, the shear storage and loss moduli of each of the dampers tested were computed and are recorded in Tables 2.2 and 2.3. These results are also plotted in Fig. 2.5 for damper #1.

In Tables 2.2 and 2.3, the values for the first column denoted by 'first cycle' were obtained from the ratio between force and displacement in the first cycle. The second column denoted by 'average' gives the average results over 15 to 20 cycles, whereas the third column quantities denoted by 'stable' were obtained from the ratio between force and displacement when the force reached a stable level. Time histories of both displacement and force as shown in Figs. 2.3 and 2.4 show that it does not take many cycles (generally 15 to 20) for the force to reach a stable value. Since dampers usually undergo many cycles in most practical applications, it is reasonable to use the stable values of G' and G'' when specifying the mechanical properties of VE dampers.

2.4 ANALYSIS OF THE EXPERIMENTAL RESULTS

We can conclude from the results given in the preceding section that the mechanical properties of VE dampers are strongly dependent on temperature. Increases in temperature can be caused by both (1)

Damper 1	First Cycle		Average		stable		δ
Temp. (°C)	G' (lb/in²)	G'' (lb/in²)	G' (lb/in²)	G'' (lb/in²)	G' (lb/in²)	G'' (lb/in²)	(DEG)
22.9	1313.3	1875.7	729.9	1054.4	517.9	739.9	55
25.5	920.0	1313.8	548.3	783.1	419.1	598.5	55
27.8	708.7	1012.2	463.5	661.9	366.1	522.9	55
31.4	465.4	664.7	345.3	493.2	289.1	412.8	55
33.1	287.1	410.1	234.2	334.5	213.3	304.7	55

Damper 1	First Cycle		Average		stable		δ
Freq. (Hz)	G' (lb/in²)	G'' (lb/in²)	G' (lb/in²)	G'' (lb/in²)	G' (lb/in²)	G'' (lb/in²)	(DEG)
0.2	449.7	619.0	369.9	509.1	338.7	466.2	56
0.5	708.7	1012.2	463.5	661.9	366.1	522.9	55
1.0	936.8	1388.8	514.5	762.8	358.4	532.1	55
2.0	1154.1	1588.4	609.2	835.5	389.2	535.7	54

TABLE 2.2. G' and G" for Damper No. 1 at Different Temperatures and Frequencies

Damper 2	First Cycle		Average		stable		δ
Temp. (°C)	G' (lb/in²)	G'' (lb/in²)	G' (lb/in²)	G'' (lb/in²)	G' (lb/in²)	G'' (lb/in²)	(DEG)
24.4	1192.9	1768.6	575.0	852.5	463.3	632.1	56
27.6	630.5	900.5	397.9	568.3	310.7	443.8	55
30.2	465.9	641.3	322.1	443.3	266.3	366.5	54
34.9	264.3	338.3	218.9	280.2	210.8	269.9	58

Damper 3	First Cycle		Average		stable		δ
Temp. (°C)	G' (lb/in²)	G'' (lb/in²)	G' (lb/in²)	G'' (lb/in²)	G' (lb/in²)	G'' (lb/in²)	(DEG)
22.8	956.2	1417.6	629.9	933.9	559.2	829.0	56
25.5	671.0	994.8	488.9	724.9	440.9	653.6	56
27.5	590.1	812.2	434.8	598.5	401.5	552.6	56
30.2	417.5	596.3	327.2	467.3	309.7	442.3	55
33.3	236.2	325.1	206.7	384.5	201.4	277.1	54

Damper 4	First Cycle		Average		stable		δ
Temp. (°C)	G' (lb/in²)	G'' (lb/in²)	G' (lb/in²)	G'' (lb/in²)	G' (lb/in²)	G'' (lb/in²)	(DEG)
27.8	439.8	670.9	359.8	513.8	338.4	483.0	55
30.0	356.8	491.1	290.3	399.6	376.3	380.2	54
34.2	21.4	282.0	191.2	353.7	189.6	251.6	53

TABLE 2.3a. G' and G" of Damper Nos. 2, 3 and 4 at Different Temperatures

Damper 5	First Cycle		Average		stable		δ
Temp. (°C)	G' (lb/in^2)	G'' (lb/in^2)	G' (lb/in^2)	G'' (lb/in^2)	G' (lb/in^2)	G'' (lb/in^2)	(DEG)
23.0	782.3	1038.2	547.2	726.1	479.2	635.9	53
27.0	410.0	544.1	321.4	426.5	293.1	389.1	54
31.0	198.8	272.8	171.3	235.8	165.0	227.1	53

Damper 6	First Cycle		Average		stable		δ
Temp. (°C)	G' (lb/in^2)	G'' (lb/in^2)	G' (lb/in^2)	G'' (lb/in^2)	G' (lb/in^2)	G'' (lb/in^2)	(DEG)
24.1	918.8	1143.6	639.7	790.0	573.9	708.7	51
28.0	551.3	731.5	414.3	549.8	380.3	504.7	53
30.4	389.9	517.7	311.5	413.4	296.1	392.9	53
33.4	231.1	285.4	204.3	252.2	196.3	242.5	51

Damper 7	First Cycle		Average		stable		δ
Temp. (°C)	G' (lb/in^2)	G'' (lb/in^2)	G' (lb/in^2)	G'' (lb/in^2)	G' (lb/in^2)	G'' (lb/in^2)	(DEG)
24.8	932.8	1237.8	606.9	805.3	542.8	720.4	53
28.2	570.4	786.4	410.3	564.6	379.6	522.6	54
30.1	460.8	634.2	347.4	484.2	323.0	447.6	54
33.4	355.1	471.2	284.0	376.9	273.8	363.4	53

TABLE 2.3b. G' and G" of Damper Nos. 5, 6 and 7 at Different Temperatures

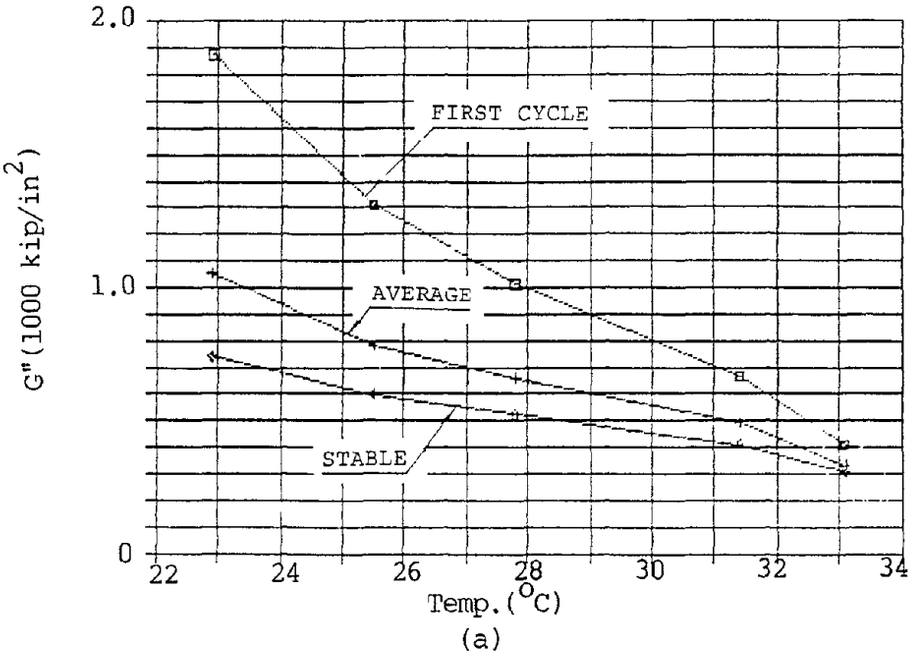

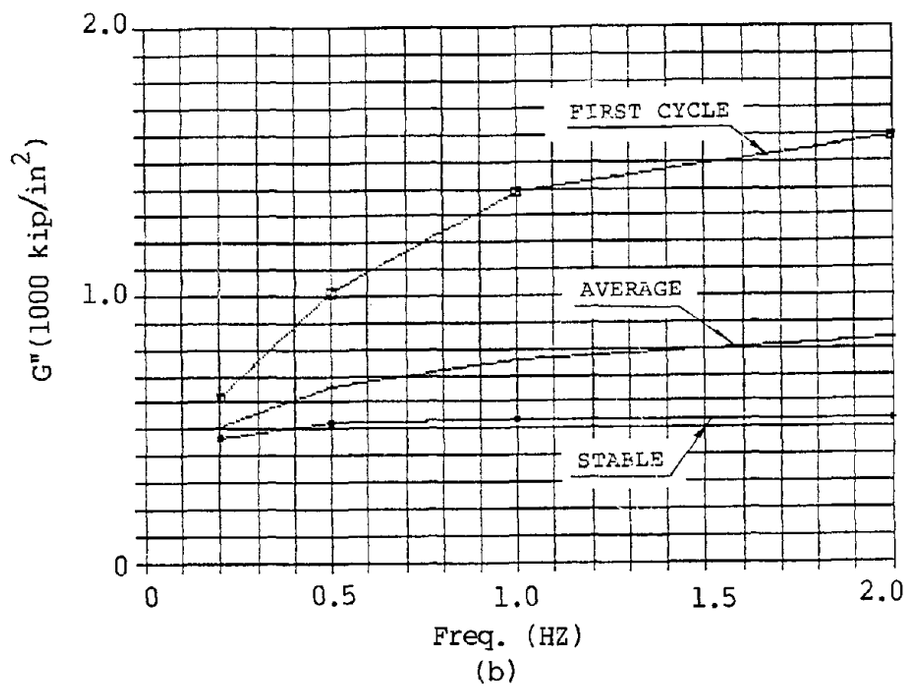

FIG. 2.5. Variations of G" with (a) Temperature and (b) Frequency

environmental temperature changes and (2) the heat generated in the damper by the conversion of vibration energy into thermal energy. Both of these factors can change the characteristics of the damper. However, temperature effect becomes negligible after several loading cycles at which time the heat generated in the damper reaches a balance with the heat radiated into the environment. The time needed to reach this equilibrium state can vary with the damper volume, the loading frequency, the environmental temperature, and so on. This can be seen in Figs. 2.3 and 2.4.

It is commonly believed that the mechanical properties of VE dampers are a function of the loading frequency. However, this is only true when considering a wide frequency range. In this test and in most civil engineering applicatons, frequency is usually considered in a relatively low and narrow range. Results of this test show that the frequency effect is not significant when the loading frequency falls into a narrow range.

SECTION 3

SINGLE-DEGREE-OF-FREEDOM SYSTEM

3.1 INTRODUCTION

Two series of structural tests were carried out using a three-story steel frame structure modeling a shear building through the method of mass simulation. In the first series, the top two floors of the model were rigidly braced to produce a single-degree-of-freedom system into which viscoelastic dampers were incorporated.

In order to provide a theoretical basis for the experiments, some theoretical considerations are first discussed.

3.2 BASIC EQUATIONS

In the following development, a linear single-degree-of-freedom system is assumed. The damping of the original structure is assumed to be small and the added damping due to the addition of VE dampers is also assumed to be small.

A system with light damping can be treated like a narrow band system [7]. When a narrow band system is excited by a wide band input (such as an earthquake, white noise, etc.), its response power spectral density function is highly concentrated near the natural frequency of the system as shown in Fig. 3.1, where S_i and S_s are, respectively, the input and system power spectrum density functions. This concentration near the natural frequency suggests that the predominant frequency components of a sample response function are contained in a relatively narrow band centered on the undamped natural frequency f_r. The beat phenomenon occurs when two harmonics are present whose frequencies are very close to each other.

Thus, the response envelope of a narrow band system can be expected to show similar characteristics. The "beat" is random in character (see

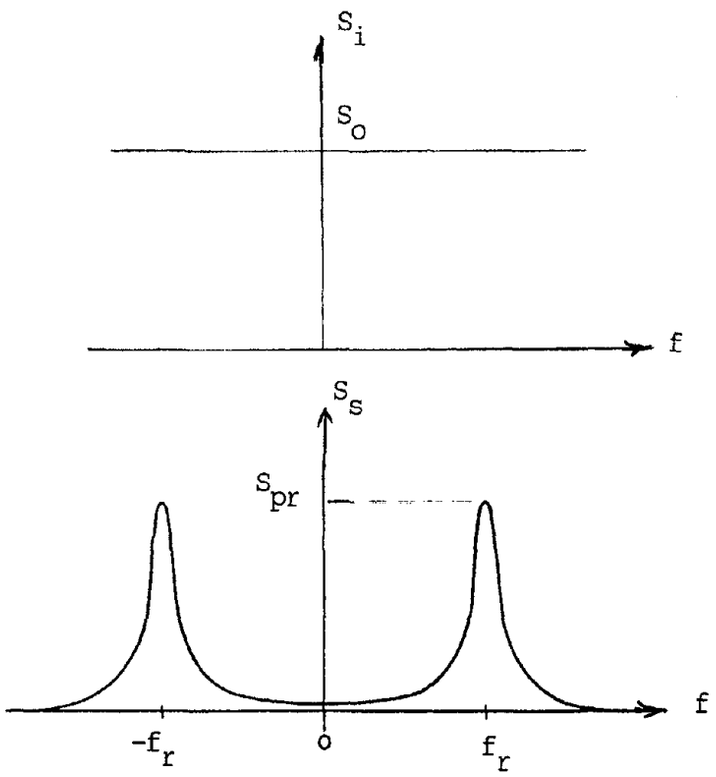

FIG. 3.1. Input and Output Spectral Density Functions

Fig. 3.2) because the predominant frequencies are spread over the narrow band. Therefore, the response of a narrow band system appears locally as a slightly distorted harmonic wave with a frequency near the system natural frequency and with amplitudes varying slowly in a random manner.

With a white noise input spectrum with level S_o, the approximate peak value of the response Bode plot can be expressed as

$$P_r = \sqrt{S_o}/2\xi k \tag{3.1}$$

and the peak value of the response power spectrum can be expressed as

$$S_{pr} = S_o/4\xi^2 k^2 \tag{3.2}$$

where ξ is the damping ratio and k is the stiffness of the system.

Since most structural systems have low damping ($\xi < 0.10$), their response to an earthquake-type input behaves like that of a narrow band system. Therefore, eqs. (3.1) and (3.2) are of practical importance.

It is seen from eqs. (3.1) and (3.2) that an increase in the damping ratio due to the presence of VE dampers reduces the peak values P_r and S_{pr}. An increase in ξ reduces P_r according to $1/\xi$ and S_{pr} according to $1/\xi^2$.

3.3 EQUIVALENT STIFFNESS AND DAMPING RATIO

The addition of VE dampers to a structure results in an increase of stiffness and damping. In the case of equivalent stiffness, consider a structural member attached to the structure at two points i_1 and i_2, the stiffness k_i between these two points can be estimated by

$$k_i = F_i/d_i \tag{3.3}$$

where F_i is the force exerted to the structural member at points i_1 and i_2 and d_i is the member deformation.

Let k_j be a known stiffness with a measurable deformation d_j. F_i and d_i can be estimated by relating these quantities to F_j and d_j through

$$k_i = r^2 k_j \tag{3.4}$$

where

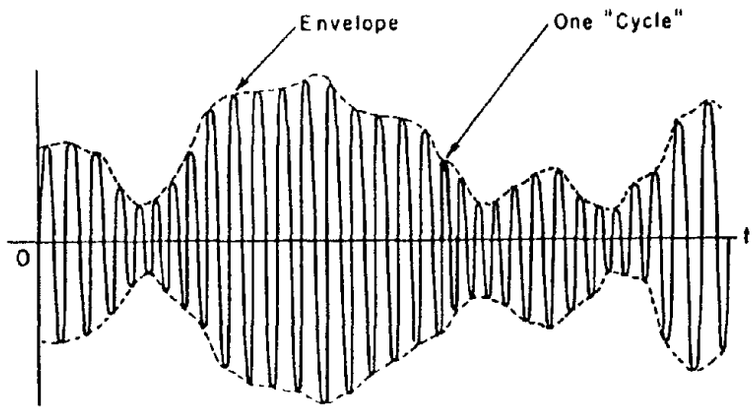

FIG. 3.2. Sample Function of a Narrow-band Process

$$r = d_j/d_i \tag{3.5}$$

For a single-degree-of-freedom system, r is a constant and is a function of the structural geometry.

The deformation ratio r can be readily found for arbitrary damper configurations. For a floor-to-wall mounting as shown in Fig. 3.3a, for example, one obtains

$$r = h/y\cos\theta \tag{3.6}$$

and, for wall-to-wall mounting (Fig. 3.3b), it takes the form

$$r = h/(y_2-y_1)\cos\theta \tag{3.7}$$

The values for r for other possible damper configurations can be similarly obtained.

Under the assumptions stated above, useful formulas can be derived for the damping ratio as well [2]. In the presence of N dampers, one can write

$$\xi = NG''A/2(k_s t + G^* A) \tag{3.8}$$

or

$$\xi = NG''A/2k_o t \tag{3.9}$$

where k_s is the structural stiffness between two mounting points of the damper and k_o is the total stiffness of the structure and the damper between the damper mounting points.

If the damper location conditions are different, eq. (3.8) or (3.9) becomes

$$\xi = G'' \sum_{i=1}^{N} \gamma_i^2 v_i / 2 \sum_{i=1}^{N} k_{oi} h_i^2 \tag{3.10}$$

where $v_i = t_i A_i$ and γ_i is the strain associated with damper i.

Equation (3.8) is useful only when k_s is available. In this series of experiments, damper design was carried out using eq. (3.9).

3.4 EXPERIMENTAL SET-UP AND RESULTS

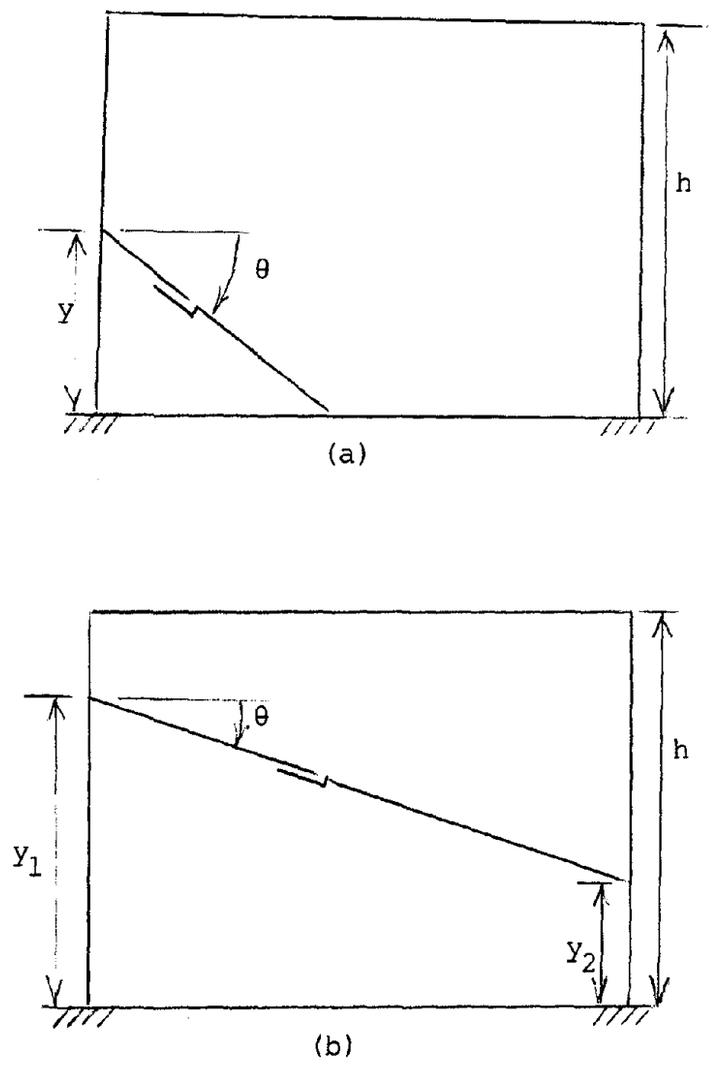

FIG. 3.3. Possible Damper Configurations

In this series of experiments, the top two floors of the model structure were rigidly braced to produce a structural system with a single degree of freedom. Two viscoelastic dampers were installed with a diagonal orientation between the first floor and the base. Fig. 3.4 shows this configuration in the laboratory and gives a close-up view of the dampers.

The structure was bolted to a concrete block which in turn was bolted to a shaking table that supplied the desired base excitation. The displacement of the first floor relative to the base was measured by a Temposonics device that was installed on a different frame which was fixed onto the table. The absolute accelerations of the first floor and the base were measured by accelerometers that were installed on the first-floor slab and on the concrete block of the base. Another Temposonics was placed on the damper to measure its relative internal displacement. Also, a thermocouple was glued to the surface of the viscoelastic material in each damper to measure damper temperature.

The data acquisition system used to monitor the experiment consisted of a minicomputer PDP11/34 with a 54-channel analog-digital converter, conditioning, amplification and low frequency filters. A spectrum analyzer was used to determine the time domain and the frequency domain response characteristics.

White noise, sine waves, and seismic motion were considered for base excitation. For seismic excitation, the N-S El Centro acceleration record was used as input, and its time history is shown in Fig. 3.5.

Some representative results in the case of seismic excitation are shown in Table 3.1. The structural parameters in this table were obtained from the absolute acceleration frequency transfer function, and the maximum response values which characterize the efficiency of the dampers were taken

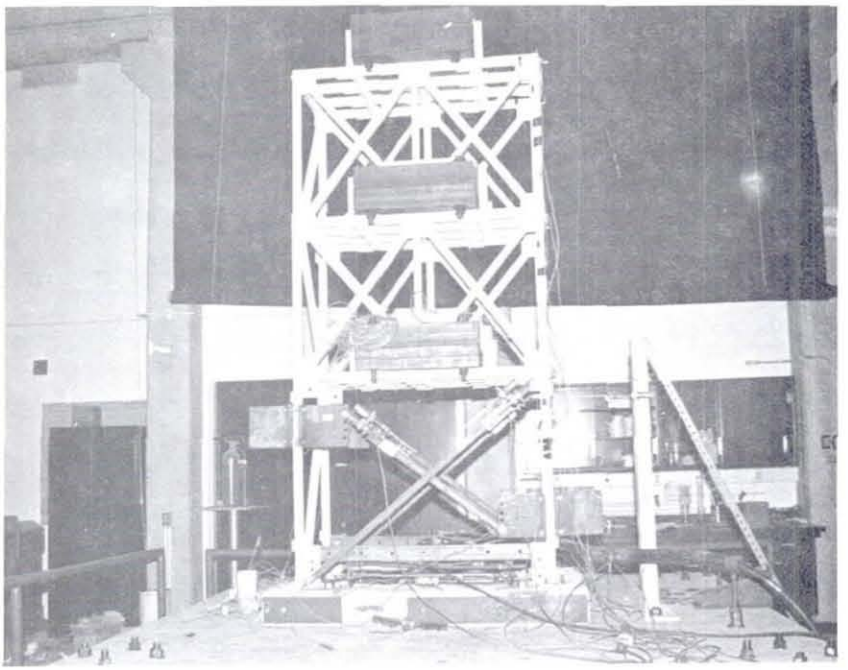

Reproduced from
best available copy.

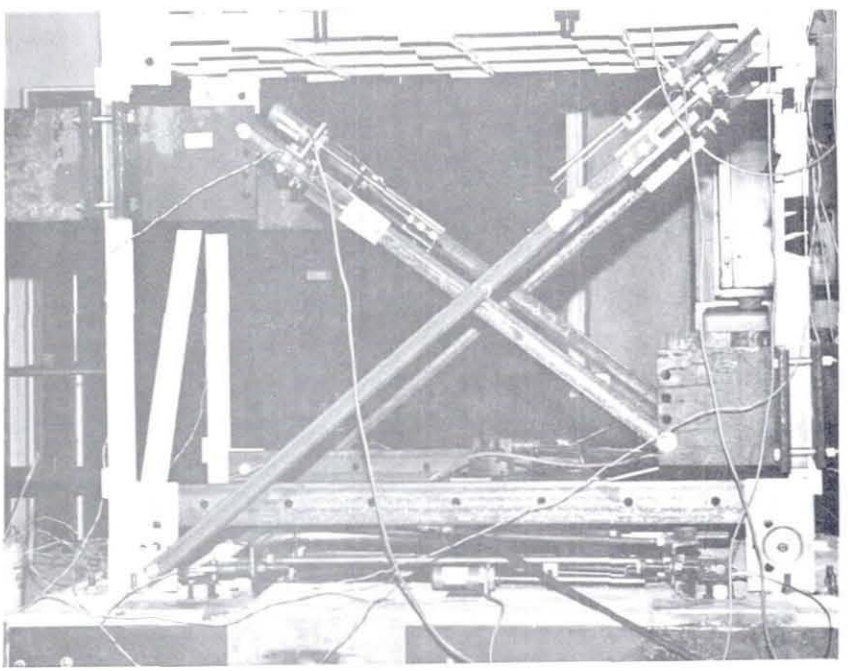

FIG. 3.4. Experimental Set-up for SDOF System

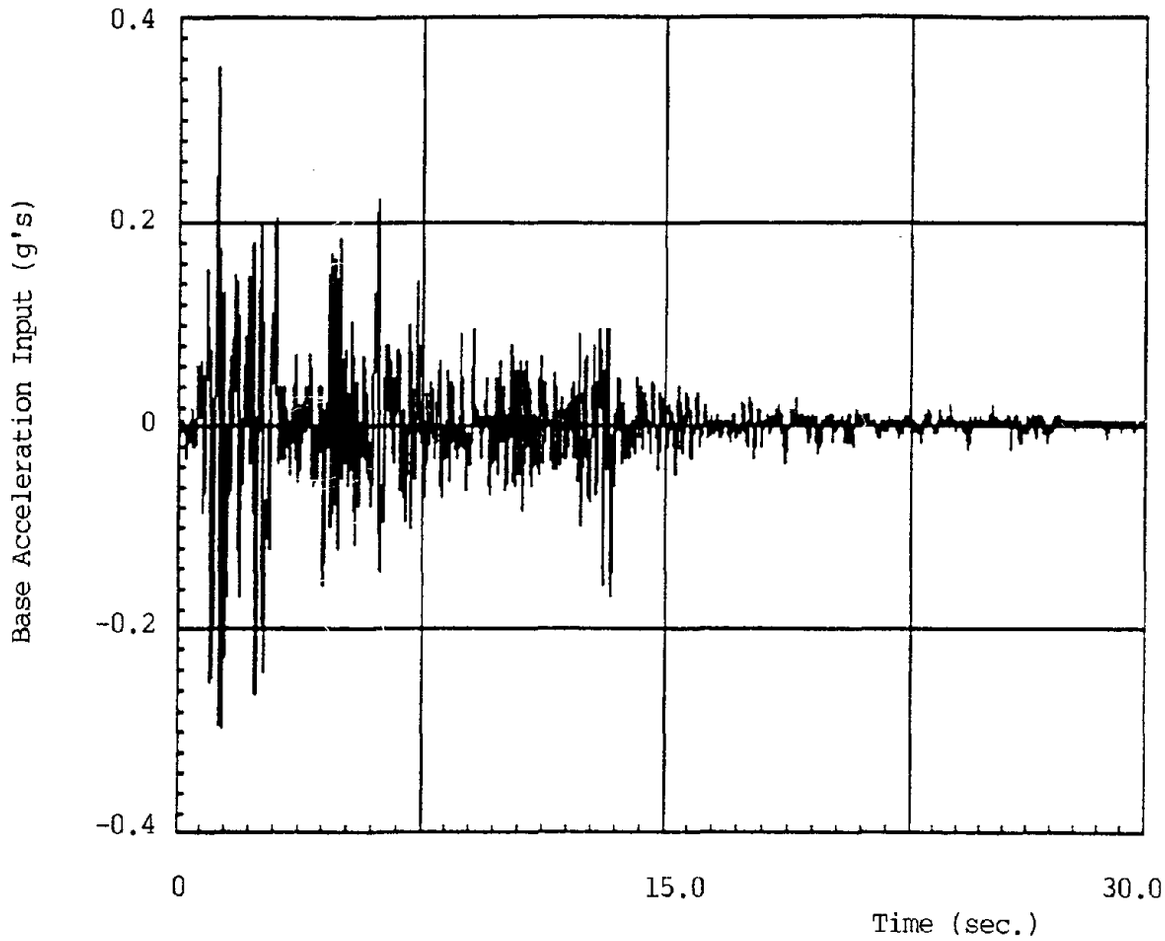

FIG. 3.5. Seismic Input for SDOF System

CASE AND TEMPERATURE	STRUCTURAL PARAMETERS		RESPONSES UNDER SEISMIC	
	NATURAL FREQUENCY	DAMPING FACTOR	Max.RELATIVE DISPLACEMENT	Max.ABSOLUTE ACCELERATION
°C	Hz	%	in	g's
NO DAMPER	5.124	4.27	0.29	1.0
WITH DAMPER				
T = 22.4	10.75	7.13	0.040	0.445
T = 26.6	9.75	18.58	0.038	0.424
T = 30.2	9.44	20.61	0.046	0.414
T = 32.0	8.63	28.62	0.047	0.412
T = 35.2	6.63	49.57	0.076	0.395

TABLE 3.1. Experimental Results - SDOF System and Seismic Input

in the time domain. Because of temperature-dependent behavior of the dampers, the results are given for different temperatures. Figures 3.6 to 3.8 show a selection of structural responses in both the time and the frequency domain. These figures were directly obtained from the spectrum analyzer for which the zero point was not compensated.

The structural system with added dampers can be compared to one without dampers. The reductions in response for the system with dampers range from 75% to 87% with respect to relative displacement and are about 60% with respect to absolute acceleration. The efficiency of the dampers can be clearly seen in Table 3.1 and Figs. 3.6-3.8.

The temperature-dependent behavior of the dampers can be seen in Table 3.1. When the temperature increases, the natural frequency decreases and the damping factor increases. Since the structural system with dampers is no longer a lightly damped system in these experiments (especially true in cases where temperature is high), the damping factors obtained from the absolute acceleration frequency transfer function are not exactly accurate. However, for purposes of relative comparison, the consistency in these data supports this general conclusion. The temperature dependency of the structural parameters can be represented graphically as shown in Figs. 3.9-3.10.

The experimental results can also be compared to results obtained from computer simulation under similar conditions and using the structural parameter values obtained in the experiment. These comparisons are summarized in Figs. 3.11-3.12. It can be seen from these figures that the simulated results closely match those obtained from the experiments.

The effect of damper configuration on structural behavior was also studied. In the one-damper case, it can be installed at different angles of inclination from the horizontal. In this set of tests, the temperature

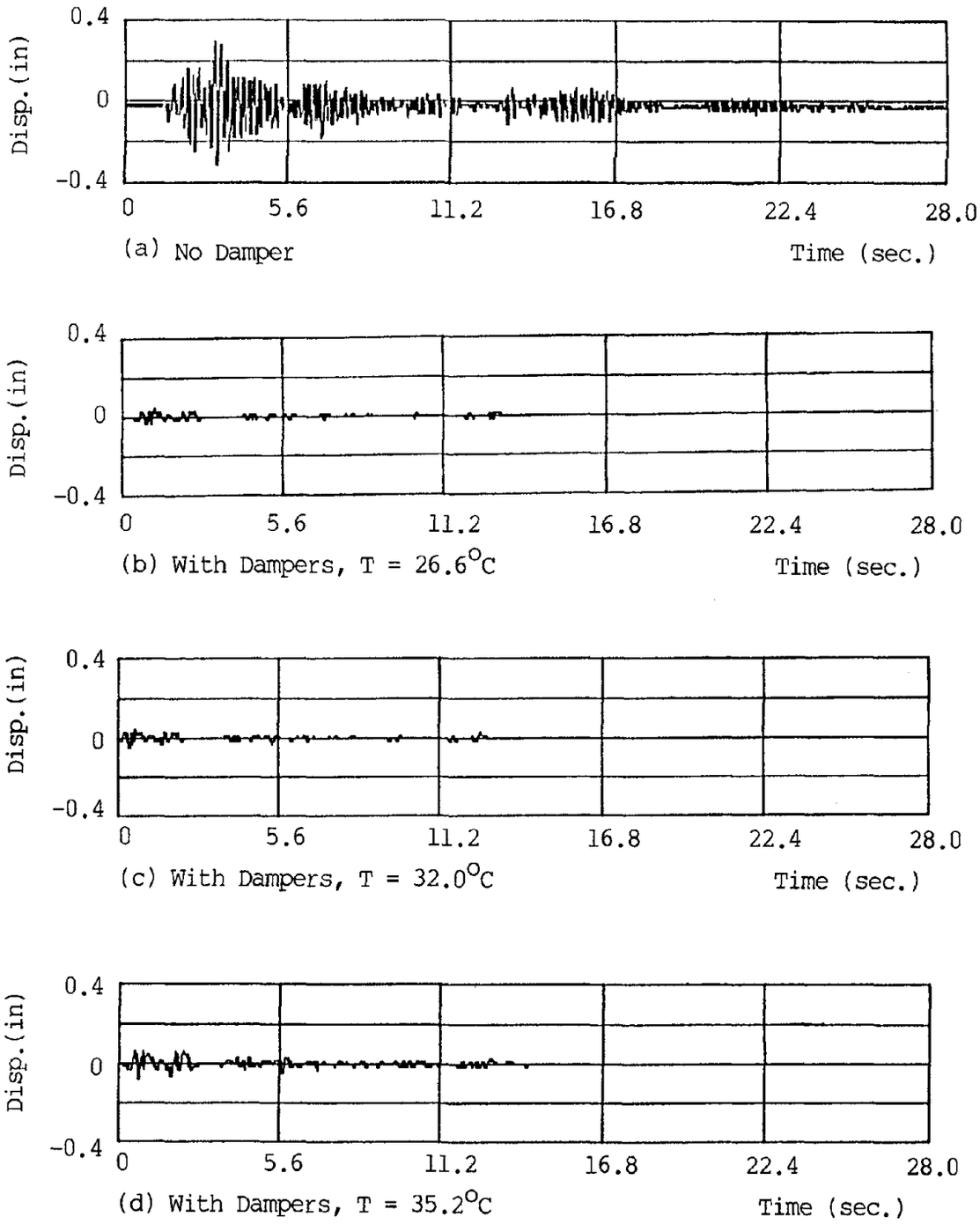

FIG. 3.6. Damper Effect on Relative Displacement

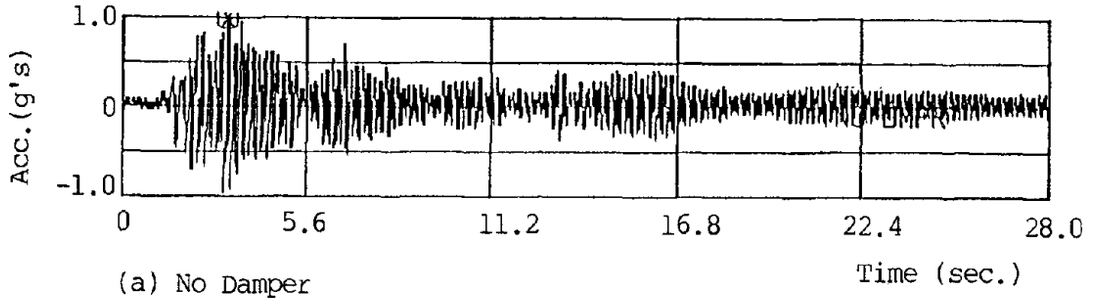

(a) No Damper

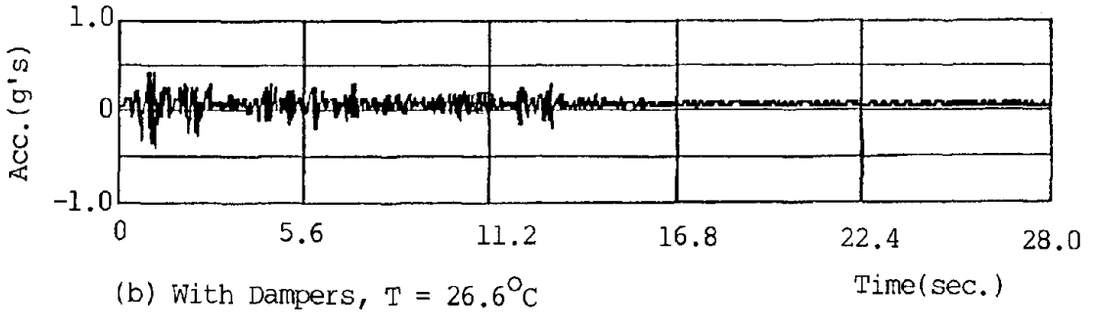

(b) With Dampers, T = 26.6°C

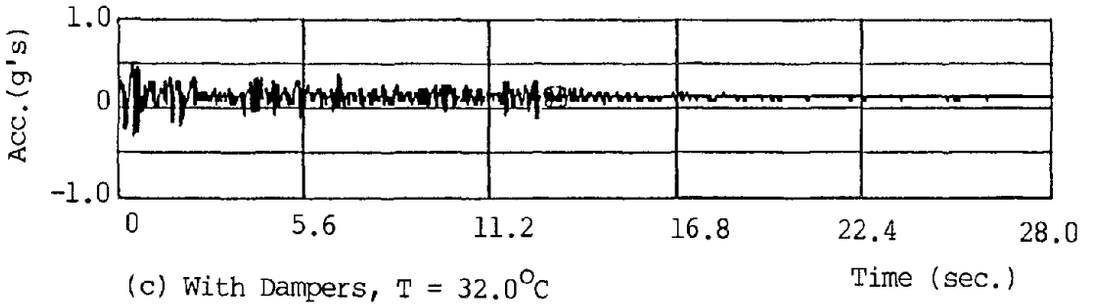

(c) With Dampers, T = 32.0°C

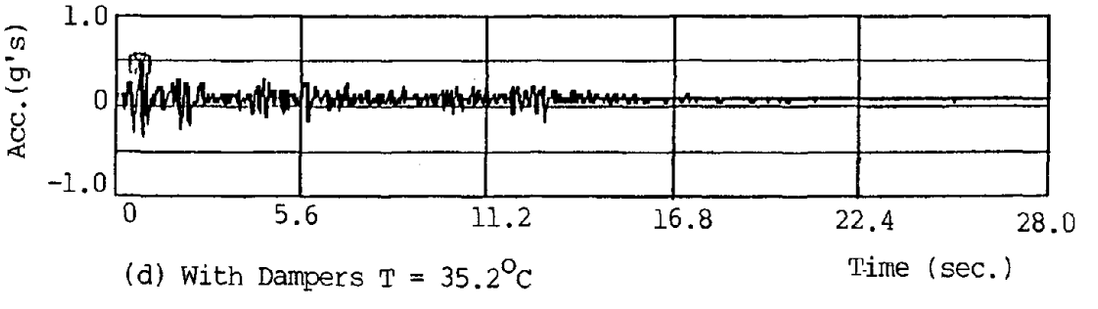

(d) With Dampers T = 35.2°C

FIG. 3.7. Damper Effect on Absolute Acceleration

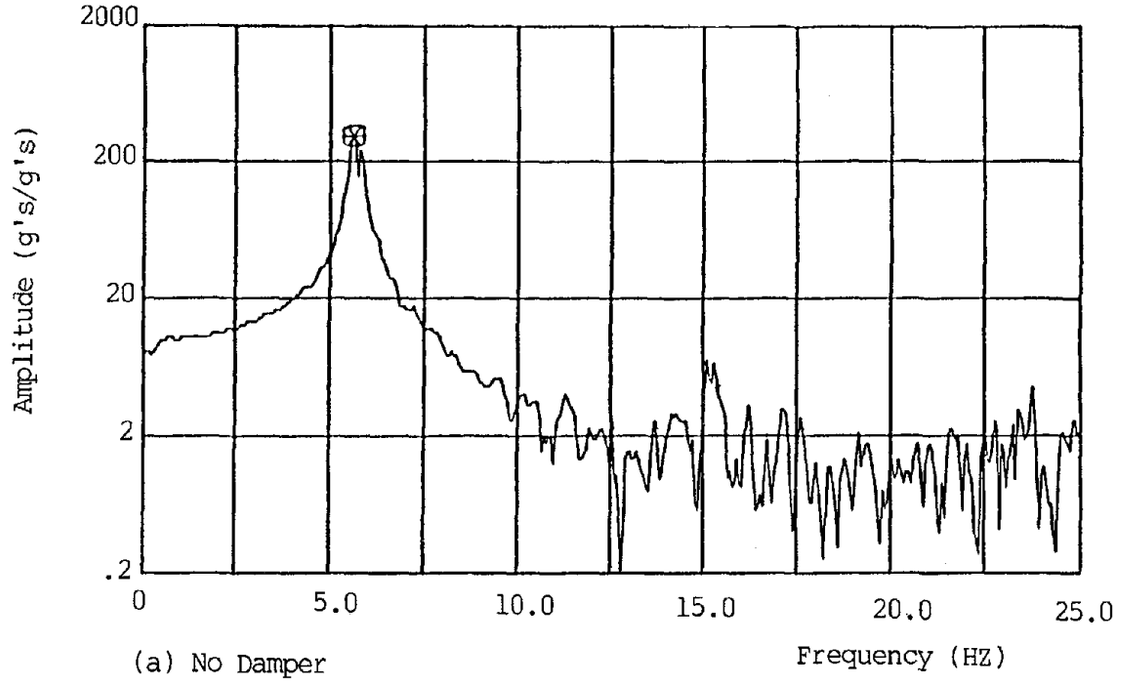

(a) No Damper

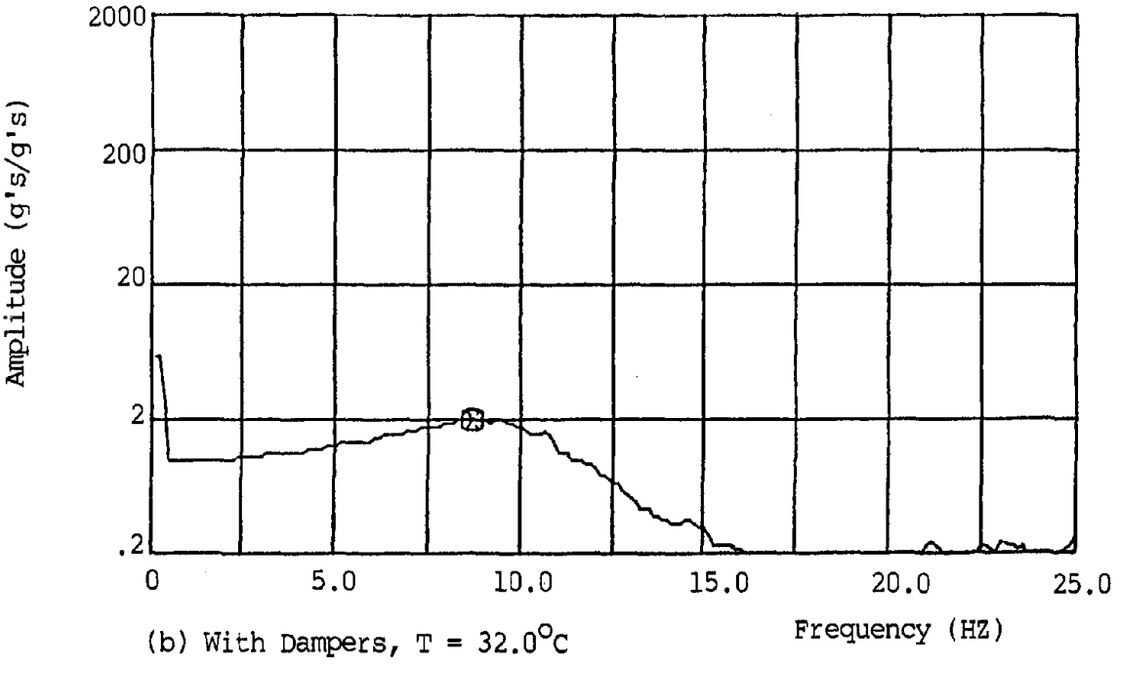

(b) With Dampers, T = 32.0°C

FIG. 3.8. Absolute Acceleration Frequency Transfer Function

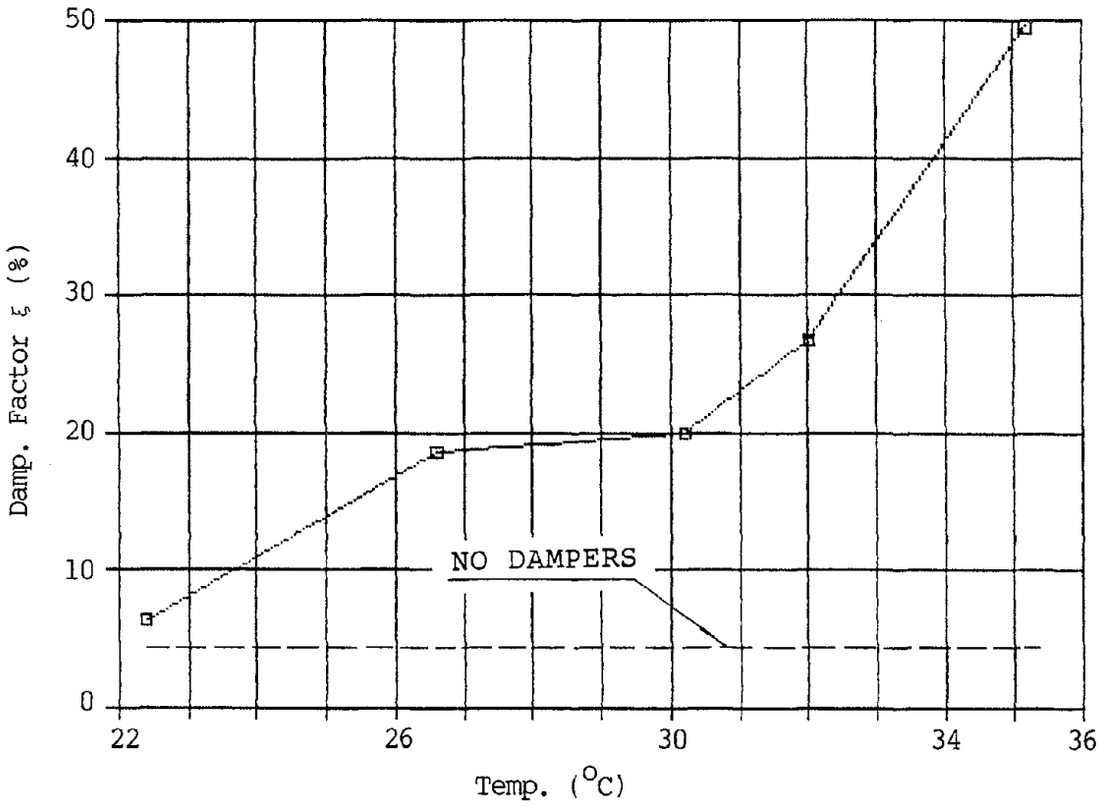

FIG. 3.9. Temperature Dependence of Damping Factor

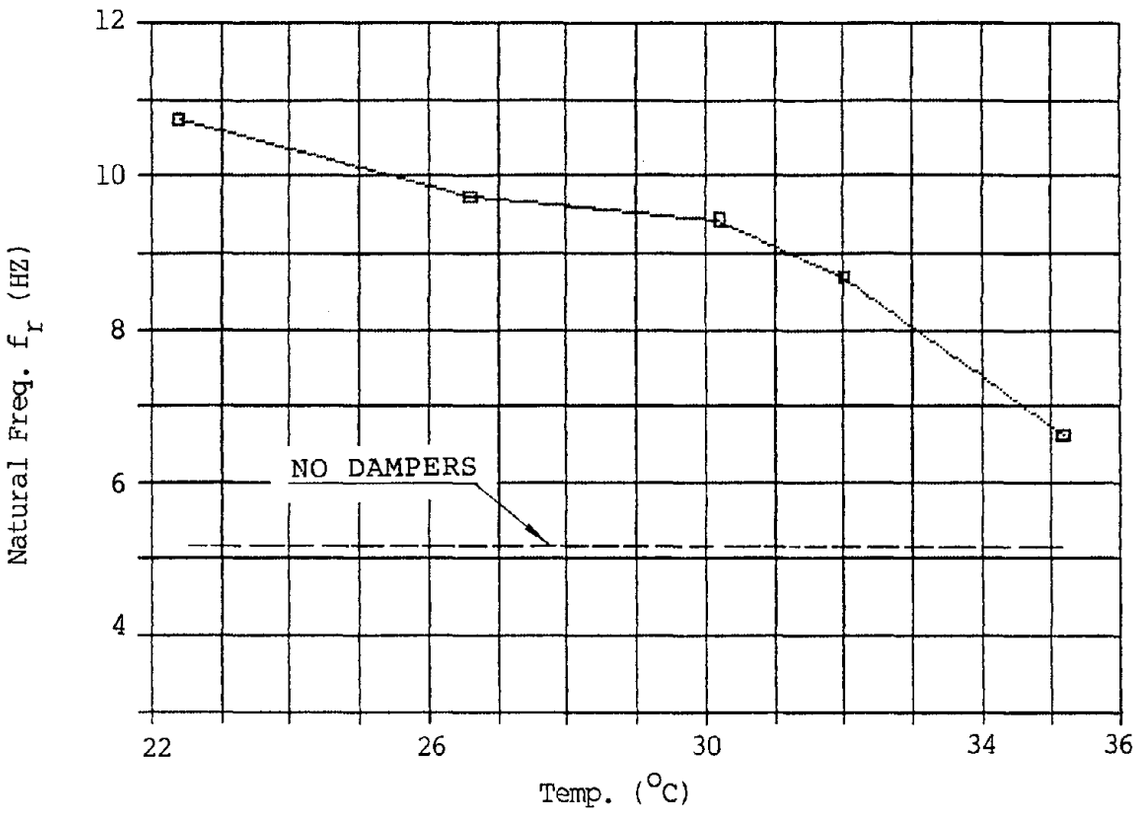

FIG. 3.10. Temperature Dependence of Natural Frequency

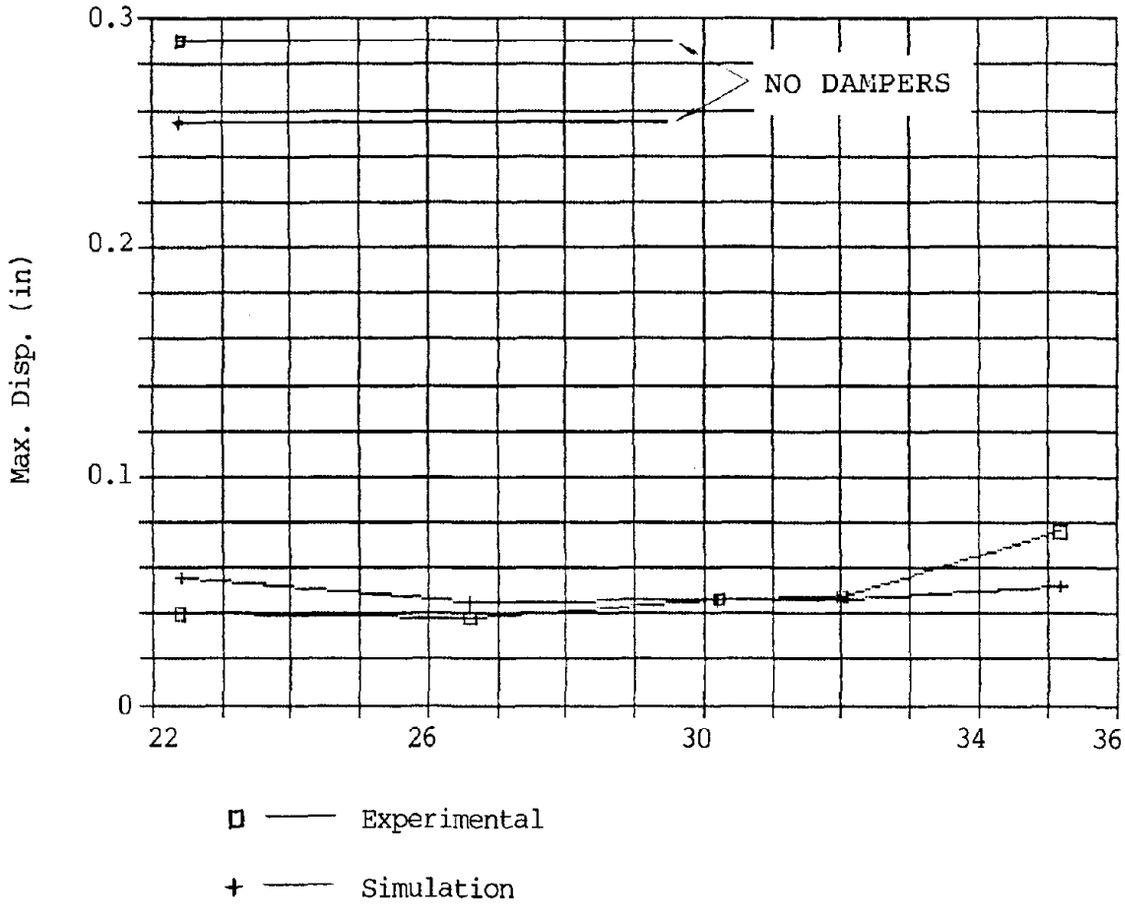

FIG. 3.11. Comparison of Experimental and Simulation Results in Maximum Relative Displacement

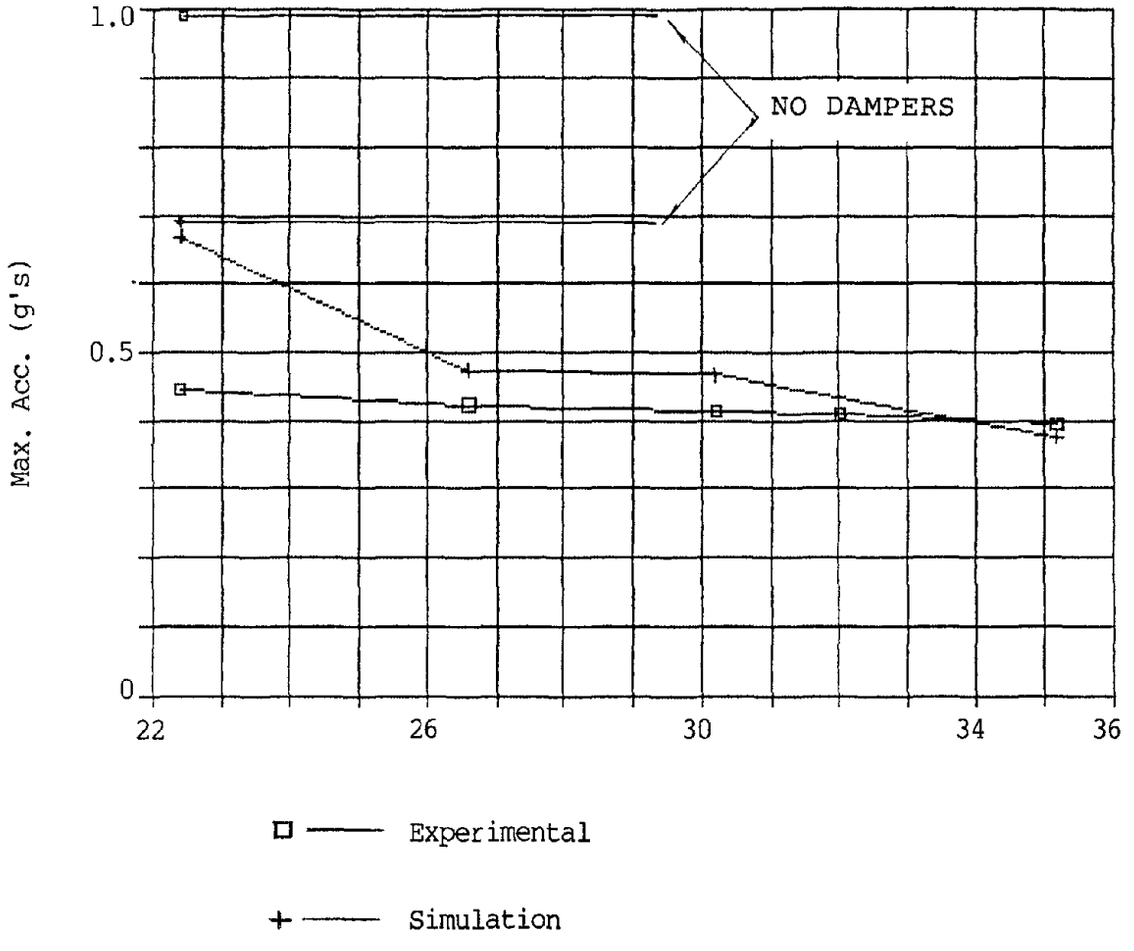

FIG. 3.12. Comparison of Experimental and Simulation Results in Maximum Absolute Acceleration

was kept at around 30^{o}C, and the results of the tests are shown in Table 3.2. The data indicate that the optimum position for a damper is in a diagonal direction. When the damper was installed in the diagonal position with an inclination angle of 37^{o} from the horizontal, the response reductions were at their maximum. This is expected since the maximum relative deformation of the structure takes place in this direction and maximum relative deformation was generated in the damper.

ANGLE FROM HORIZONTAL	TEMPERATURE	STRUCTURAL PARAMETERS		RESPONSES UNDER SEISMIC	
		NATURAL FREQUENCY	DAMPING FACTOR	Max.RELATIVE DISPLACEMENT	Max.ABSOLUTE ACCELERATION
Degree	°C	Hz	%	in	g's
12.1° 15.5°	29.6 29.5	3.19 3.62	10.78 9.83	0.10 0.097	0.094 0.148
*37.0°	26.6 29.8** 32.9	7.75 6.66 5.56	10.49 22.94 35.39	0.018 0.020 0.021	0.161 0.126 0.09
52.0° 71.0°	30.1 30.2	5.19 3.56	16.87 12.72	0.035 0.085	0.106 0.111

*Diagonal Direction between First Floor and Base

**Data obtained by Interpolation

TABLE 3.2. Results for Different Damper Configurations

SECTION 4

MULTIPLE-DEGREE-OF-FREEDOM SYSTEM

4.1 EXPERIMENTAL SET-UP

The structural model and the basic experimental facilities used in this phase of the experiments are the same as those described in Section 3, except that the rigid braces on the top two floors were removed to simulate a three-degree-of-freedom system. It thus provided more flexibility in the placement of VE dampers in a more realistic setting. Figure 4.1 shows one of the placement schemes in which VE dampers were installed on every floor.

The displacements of each floor were measured with respect to a metal frame that was not in contact with the shaking table. Instead, the frame was fixed to the floor of the laboratory so that all displacement measurements would be absolute measurements.

In this investigation, banded white noise (0-25 Hz) and seismic excitation were used as inputs. An N-S El-Centro acceleration record at 25% amplitude was used for the seismic excitation.

With respect to damper configurations, three possibilities were investigated. In case 1, a damper was installed on each floor as shown in Fig. 4.1. In case 2, a damper was installed on the first and second floors and in case 3, damper was only added to the first floor.

In consideration of temperature dependency of the viscoelastic material, experiments were performed at two different temperatures, one at the ambient temperature of approximately 23^{o}C and the other, about 30^{o}C.

4.2 EXPERIMENTAL RESULTS AND DISCUSSION

Some typical responses of the structure to seismic excitation are shown in Figs. 4.2-4.7. Figures 4.2-4.4 give the responses in the time domain while Figs. 4.5-4.7 give the responses in the frequency domain. In

Reproduced from
best available copy.

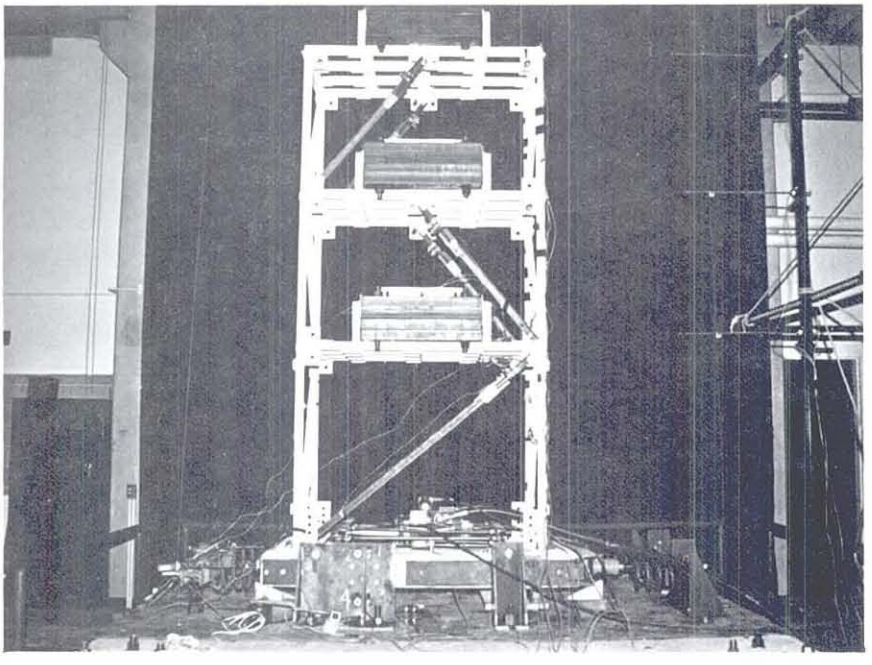

FIG. 4.1. Experimental Set-up - MDOF System

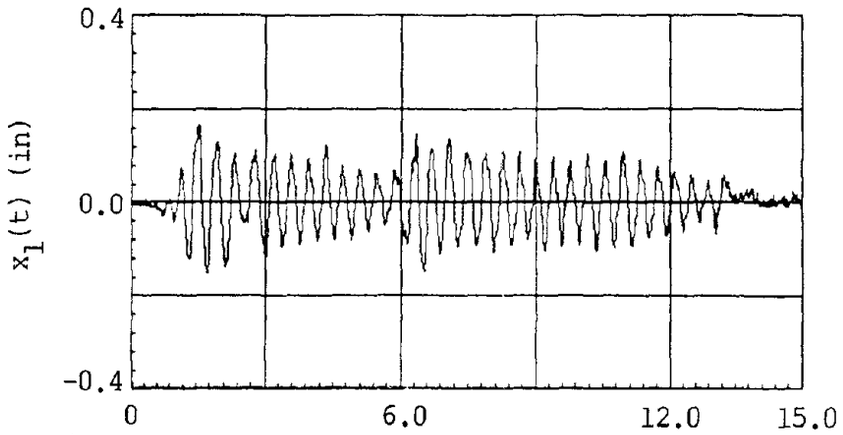

a) No Damper

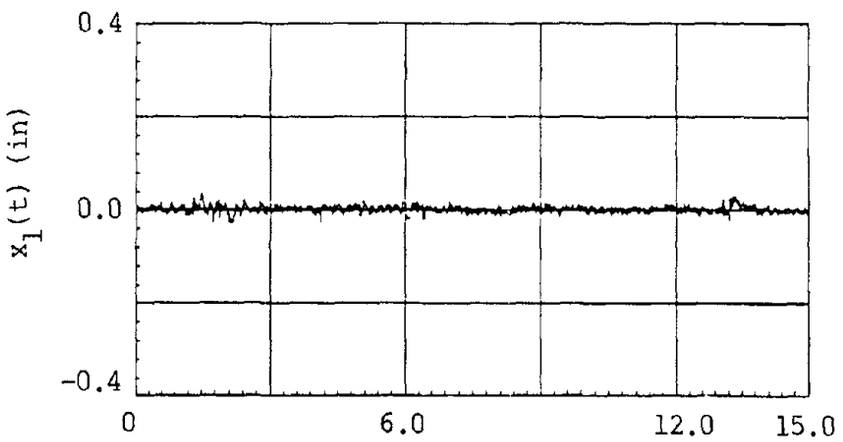

b) With Dampers, T = 22.2°C

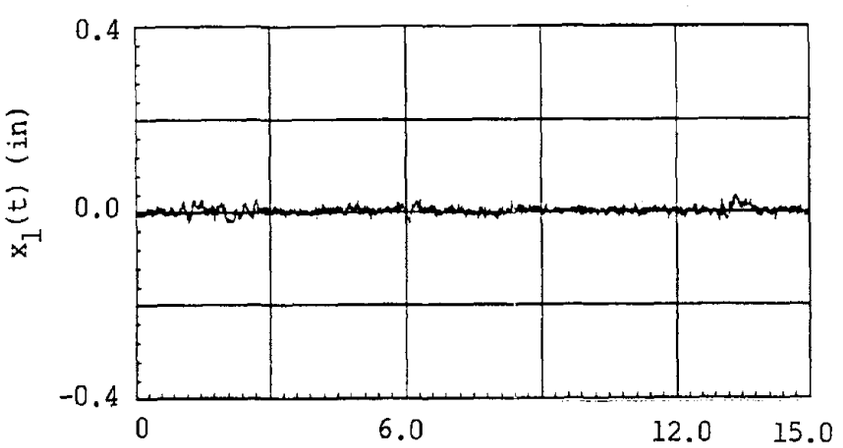

c) With Dampers, T = 27.5°C

FIG. 4.2. First-floor Relative Displacement for Case 1

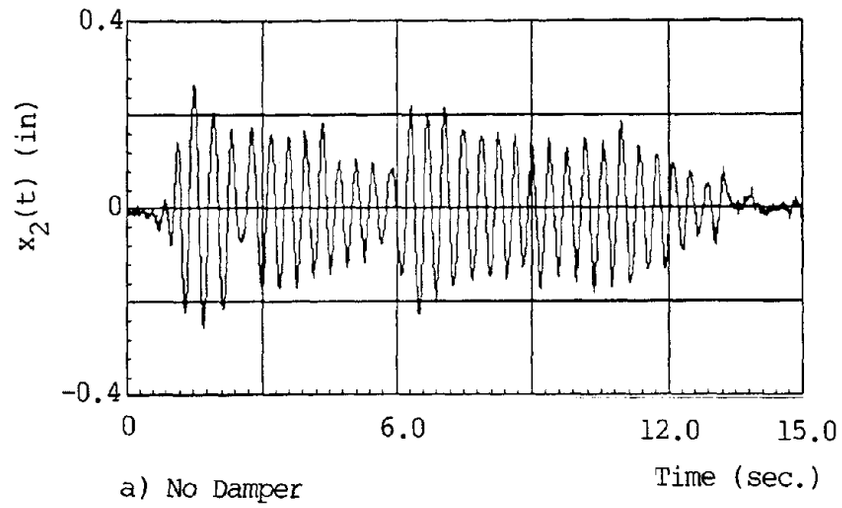

a) No Damper

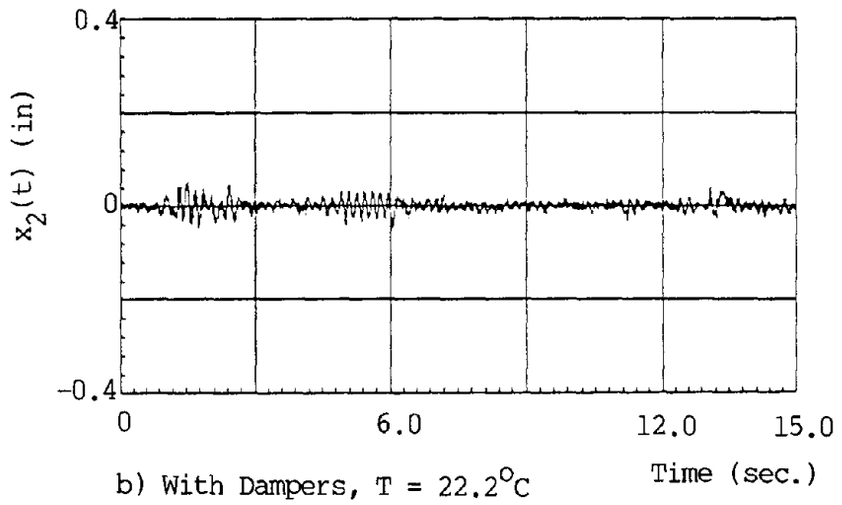

b) With Dampers, T = 22.2°C

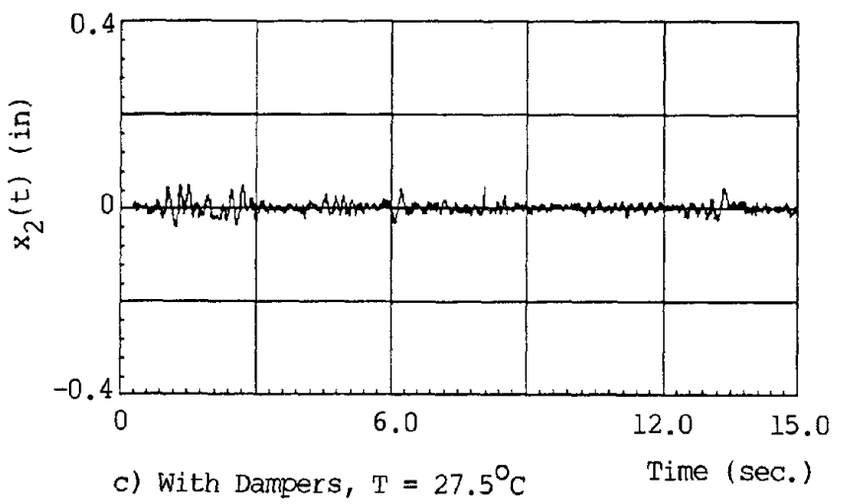

c) With Dampers, T = 27.5°C

FIG. 4.3. Second-floor Relative Displacement for Case 1

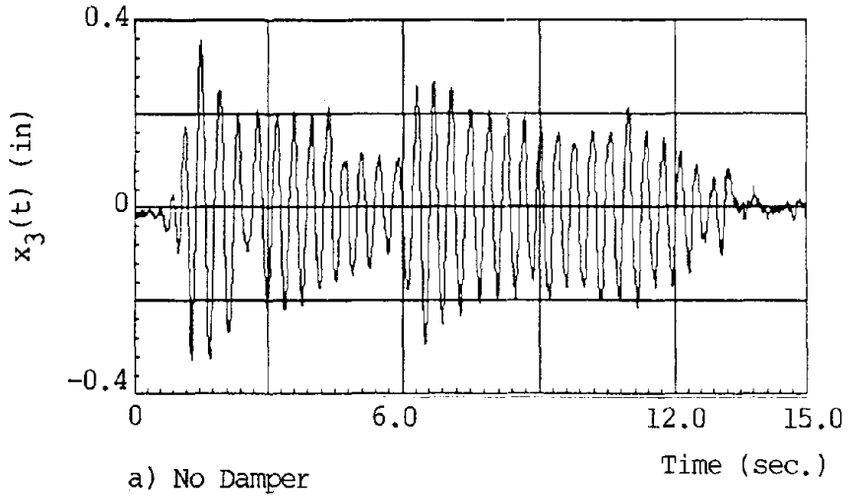

a) No Damper

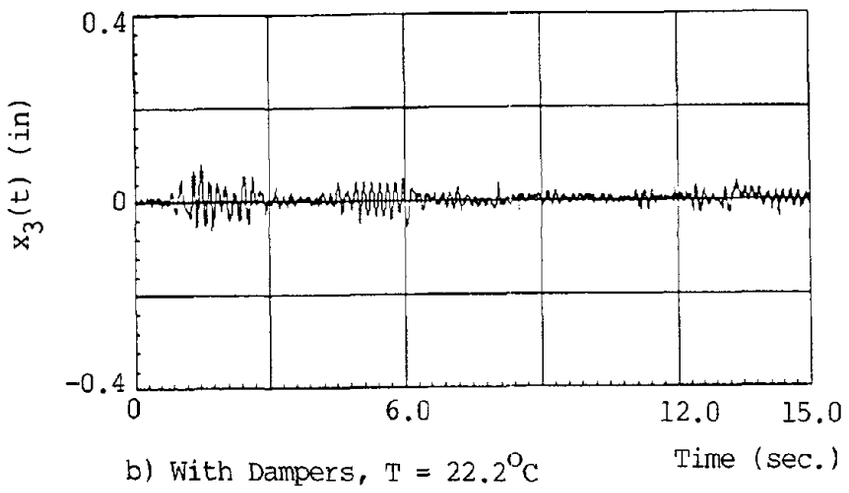

b) With Dampers, T = 22.2°C

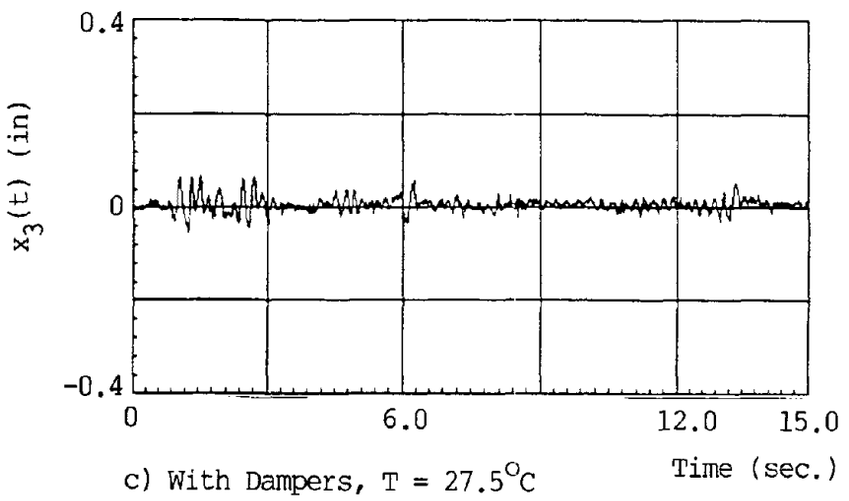

c) With Dampers, T = 27.5°C

FIG. 4.4. Third-floor Relative Displacement for Case 1

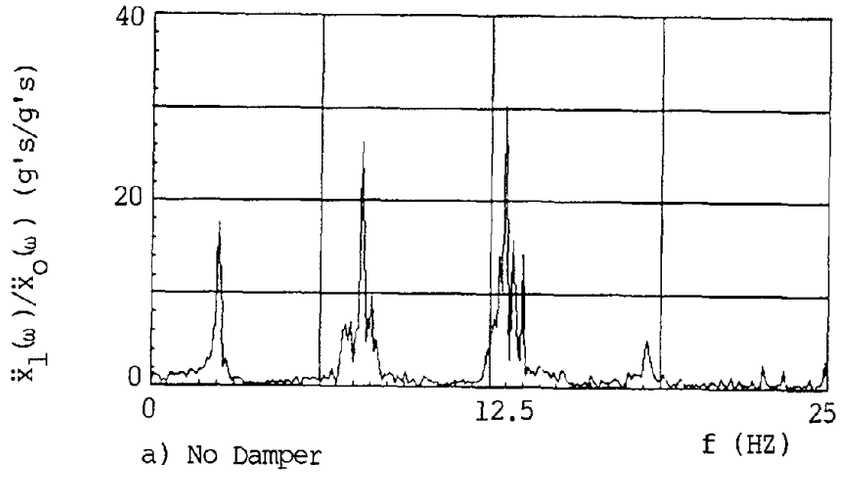

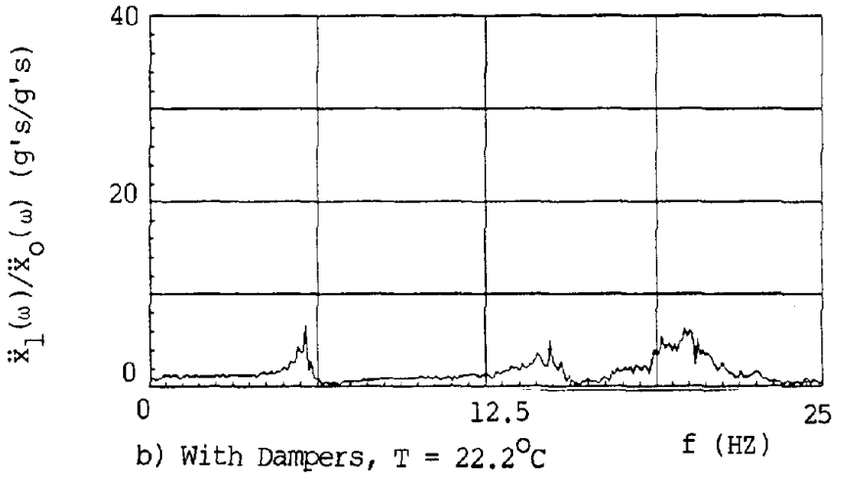

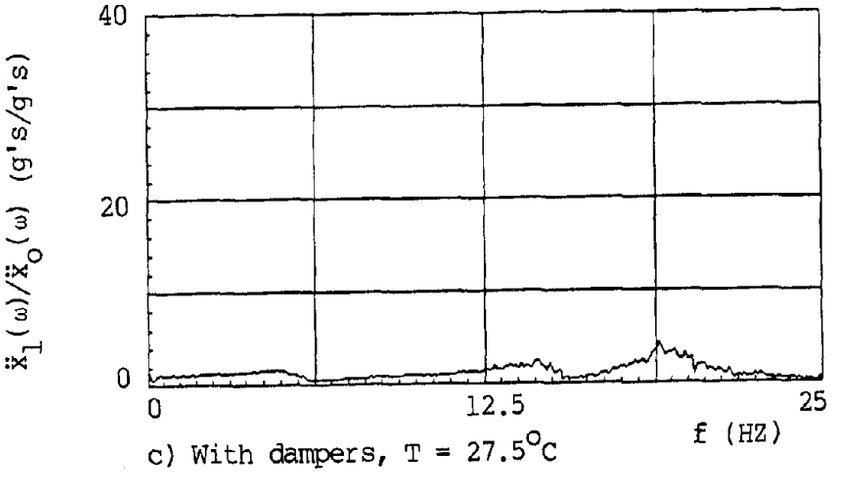

FIG. 4.5. First-floor Absolute Acceleration Frequency Transfer Function for Case 1

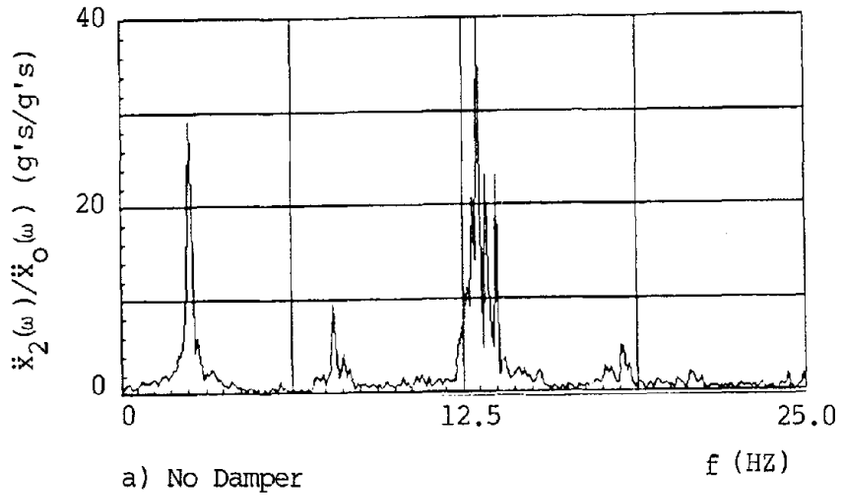

a) No Damper

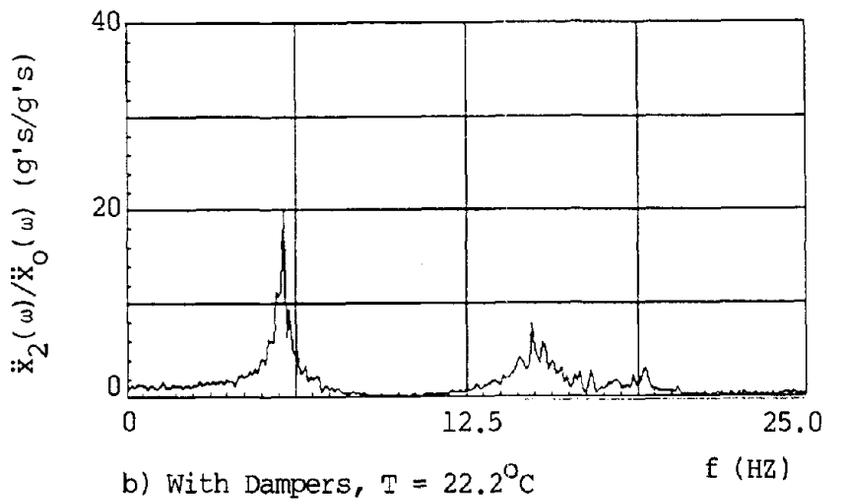

b) With Dampers, T = 22.2°C

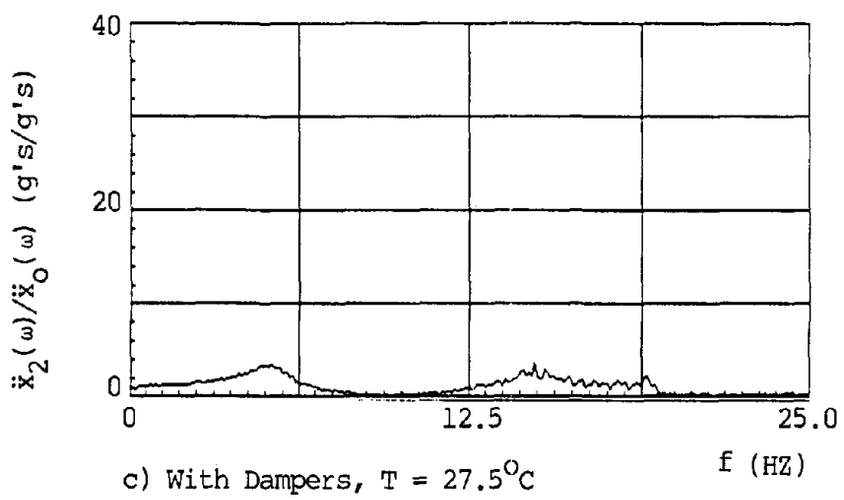

c) With Dampers, T = 27.5°C

FIG. 4.6. Second-floor Absolute Acceleration Frequency Transfer Function for Case 1

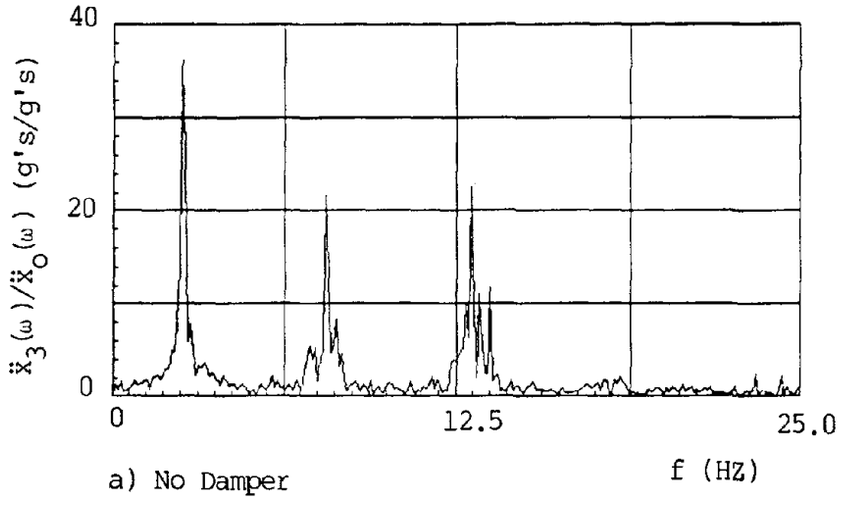

a) No Damper

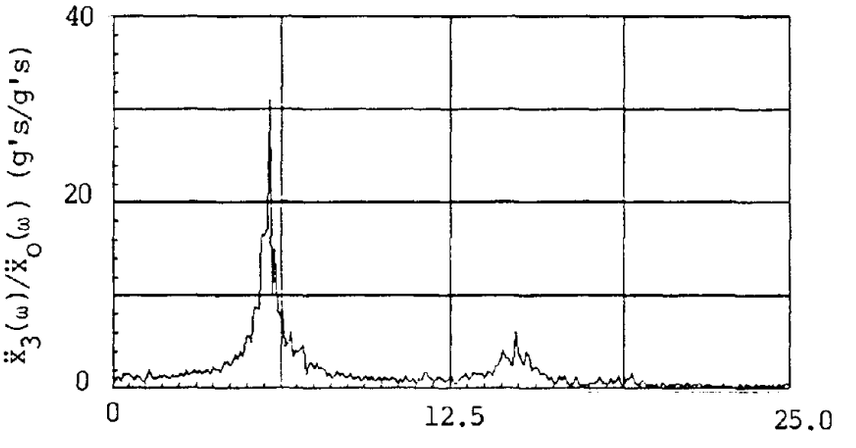

b) With Dampers, T = 22.2°C

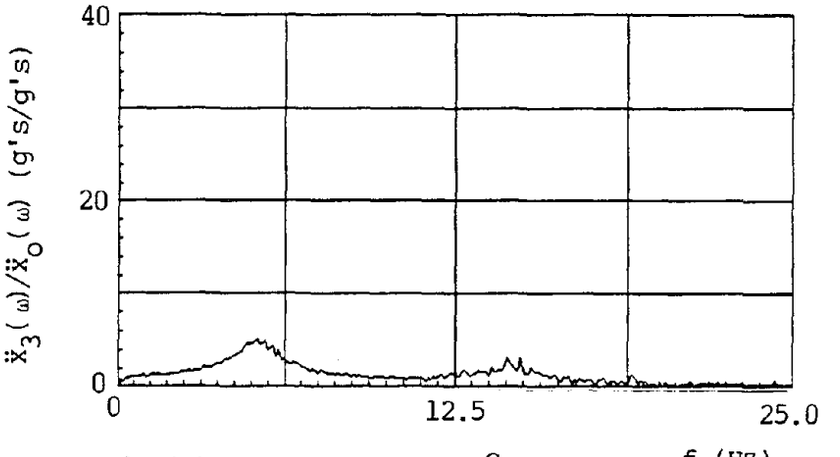

c) With Dampers, T = 27.5°C

FIG. 4.7. Third-floor Absolute Acceleration Frequency Transfer Function for Case 1

each case, the maximum value in the time domain is used to characterize the efficiency of the dampers, and a comparison of these maximum values among all cases is shown in Table 4.1. The values of the structural parameters as determined from the experimental results for each configuration at each temperature are given in Table 4.2.

The experimental results were again compared to computer simulation results using experimentally determined structural parameters. Such a simulated computation was done for each experimental case, and the results are summarized in Table 4.3. Some typical time histories for the relative displacement in each experimental case and corresponding computer simulation are shown in Figs. 4.8-4.13.

In comparing the experimental and simulated computation results, it is seen that, even though there are differences in the peak values for the amplitudes, Figs. 4.8-4.13 show a good pattern of consistency. From these figures and Tables 4.2 and 4.3, it can be seen that the simulated results consistently give lower amplitudes than the experimental results. This is most likely due to the fact that the damping factors of the structural model were probably overestimated in the simulated computation. What was not taken into account was the transformation of the structural model from a symmetrical to an unsymmetrical configuration with the addition of dampers. This may explain the fact that the response frequency transfer function did not produce just one peak around the natural frequency as seen in Figs. 4.5-4.7. Since the damping factors were overestimated, the modal shapes could only be approximated. Hence, the responses in the simulated computation were underestimated. Moreover, since the modal shapes could only be approximated, errors were unavoidable in the matrix calculations for the stiffness and damping in the simulated structural system. Since these matrices were used to determine the absolute acceleration in the

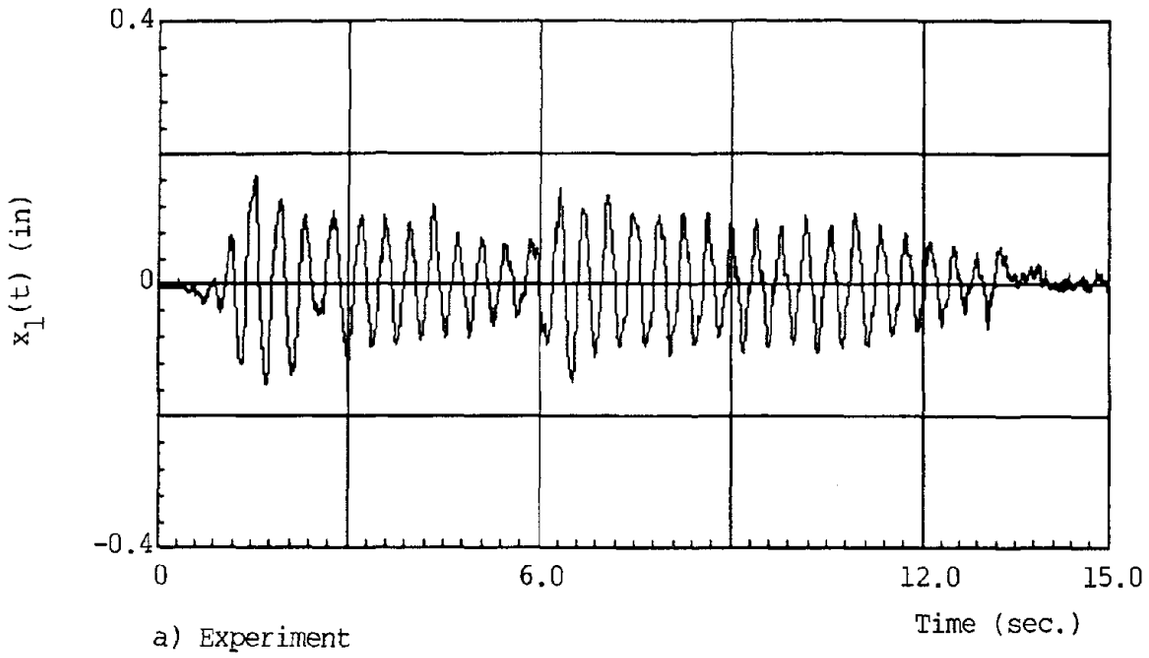

a) Experiment

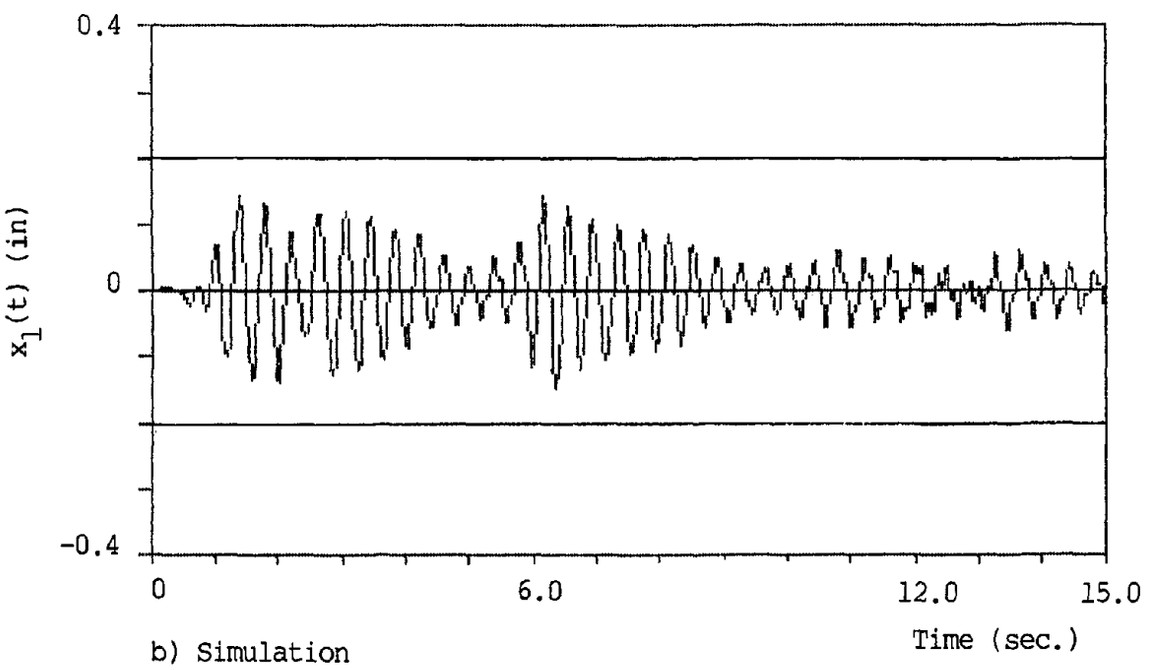

b) Simulation

FIG. 4.8. First-floor Relative Displacement (No Damper)

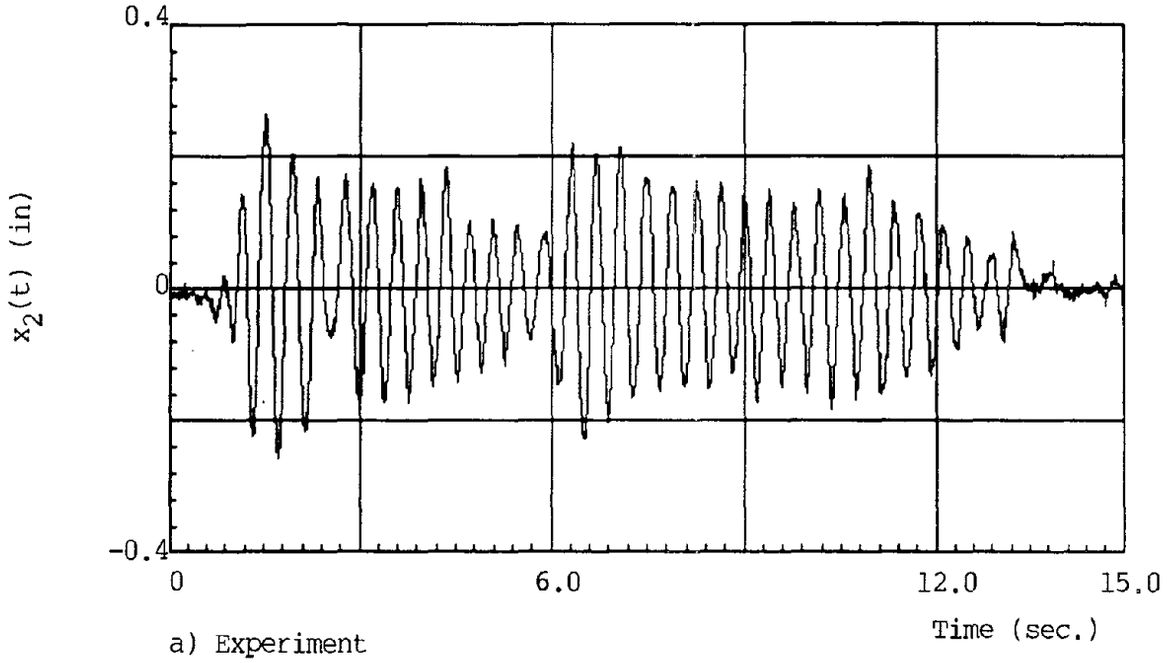

a) Experiment

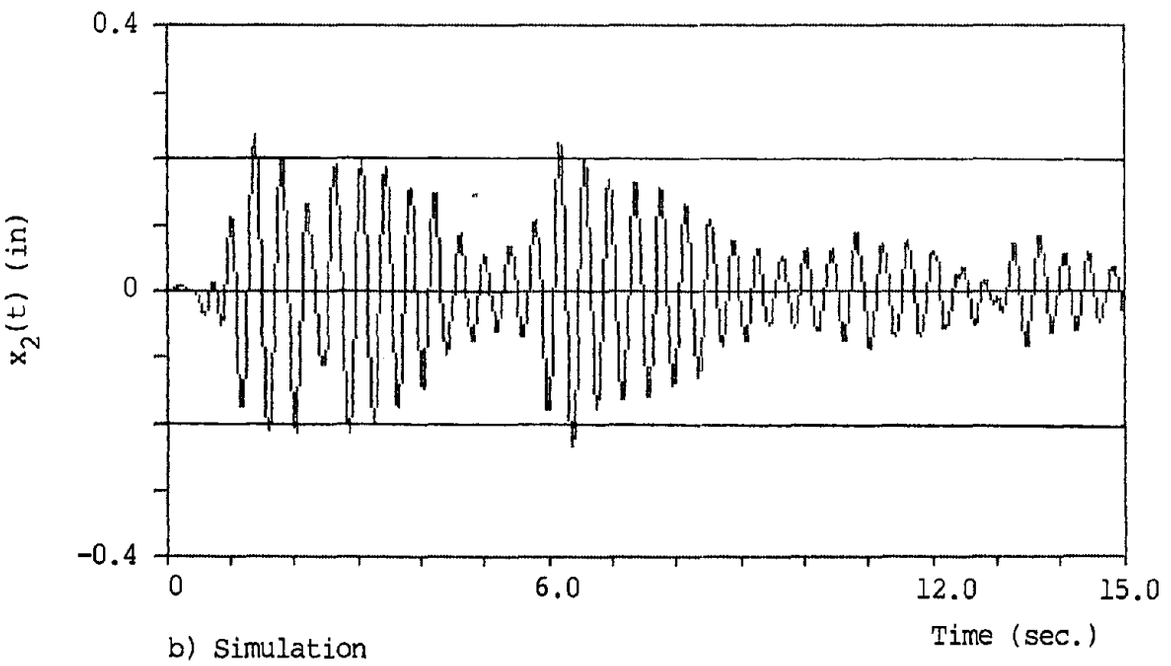

b) Simulation

FIG. 4.9. Second-floor Relative Displacement (No Damper)

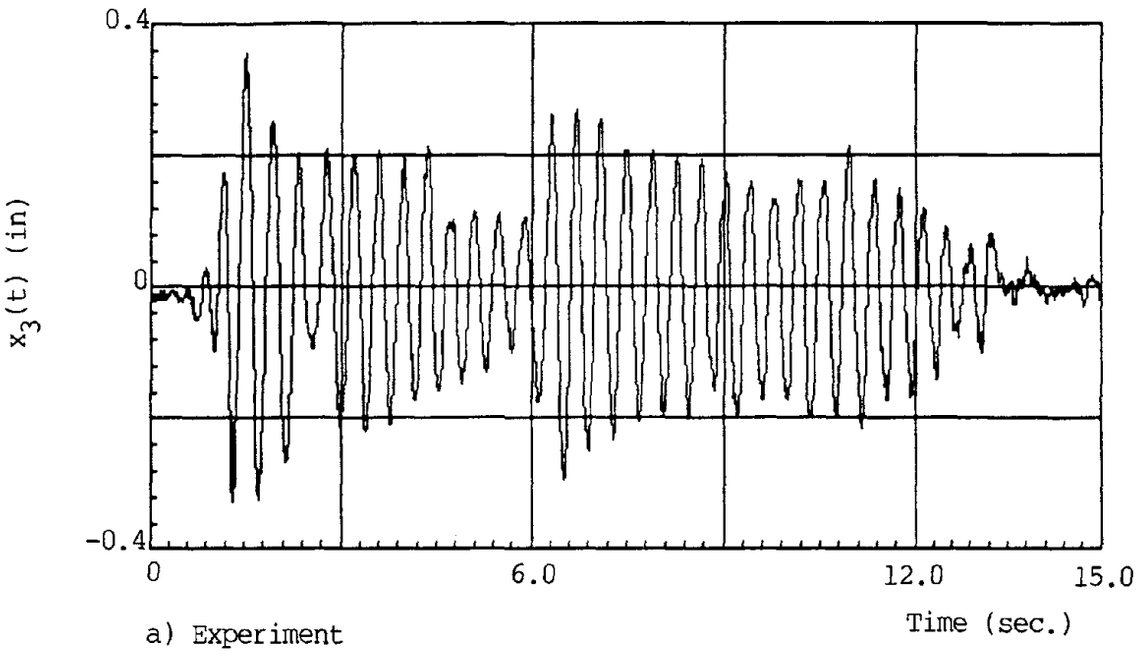

a) Experiment

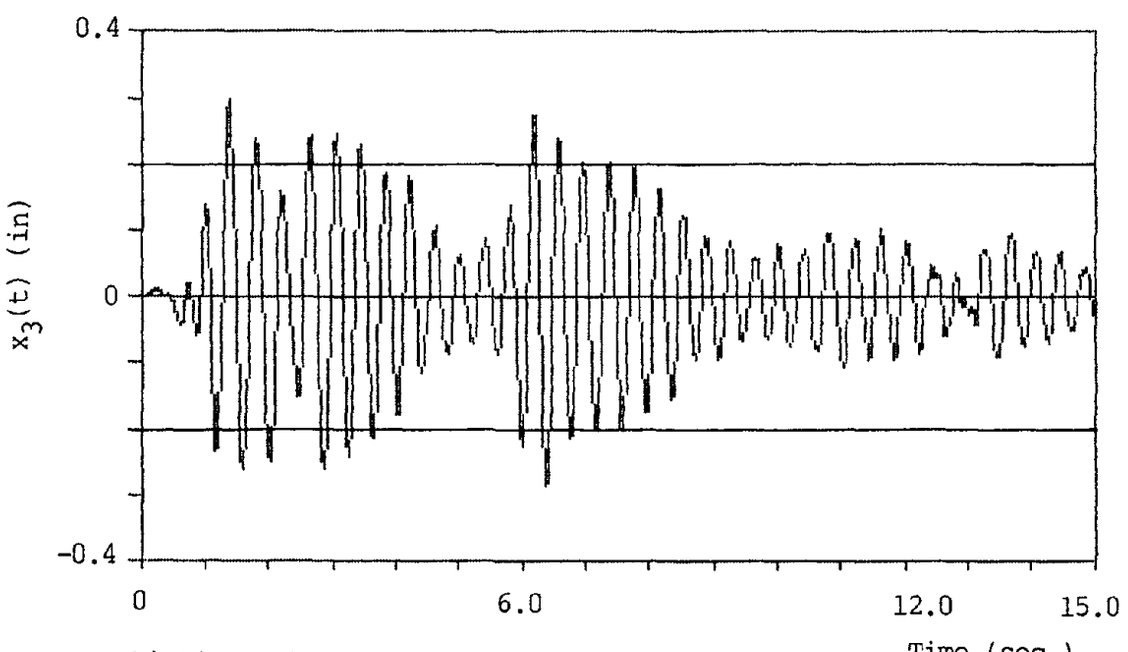

b) Simulation

FIG. 4.10. Third-floor Relative Displacement (No Damper)

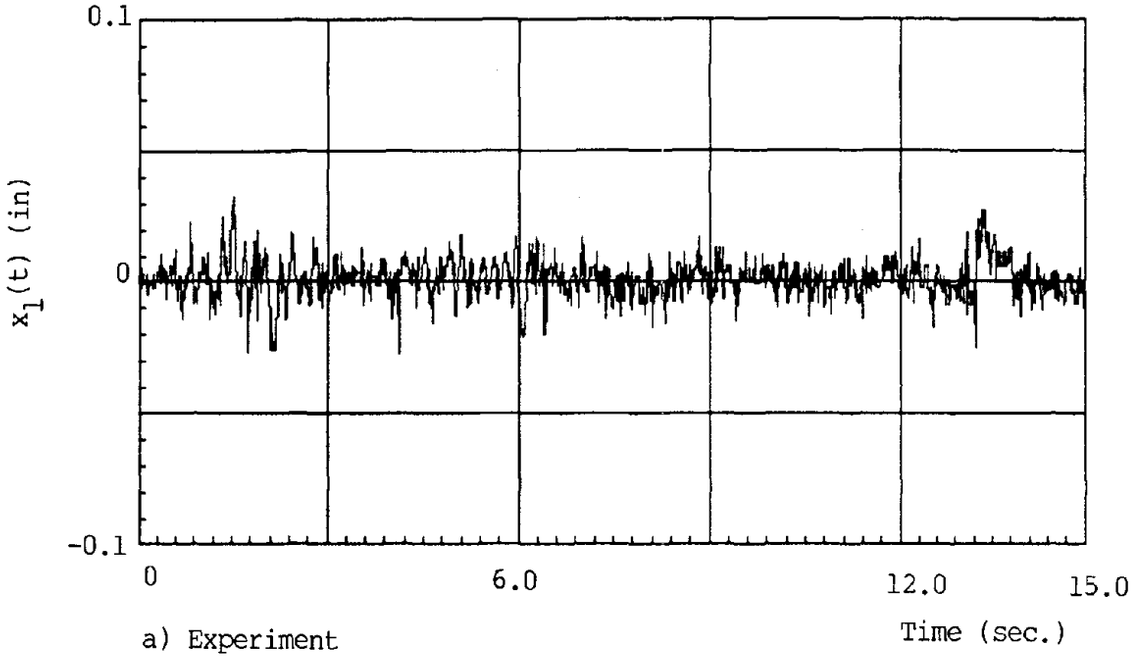

a) Experiment

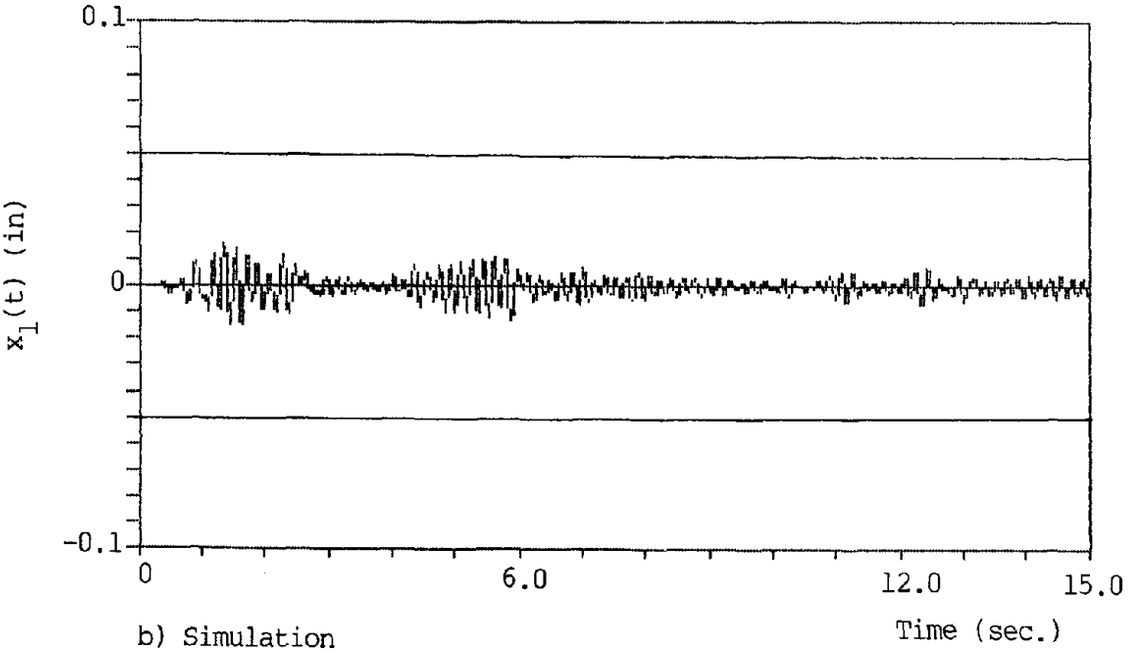

b) Simulation

FIG. 4.11. First-floor Relative Displacement for Case 1 ($T = 22.2^{\circ}C$)

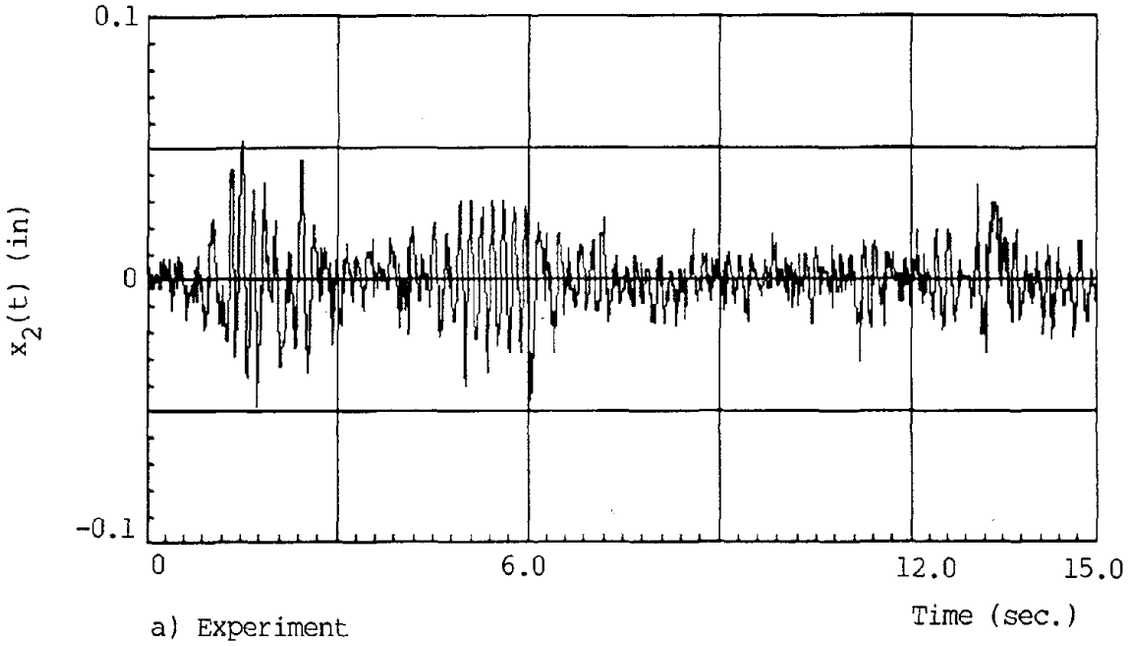

a) Experiment

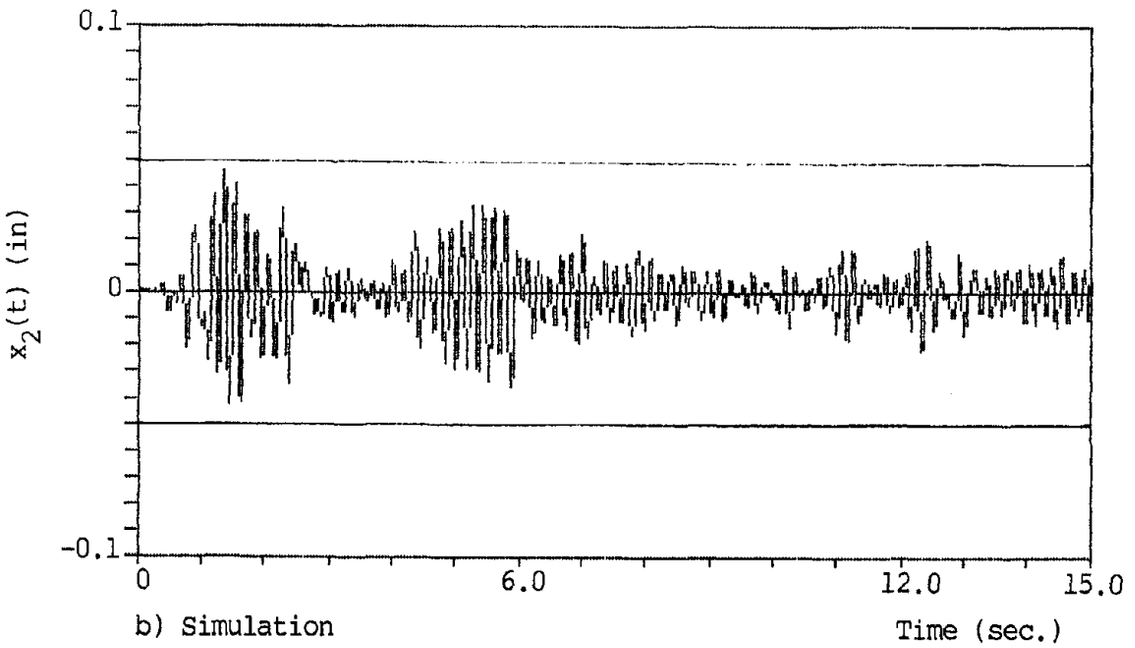

b) Simulation

FIG. 4.12. Second-floor Relative Displacement for Case 1 ($T = 22.2^{o}C$)

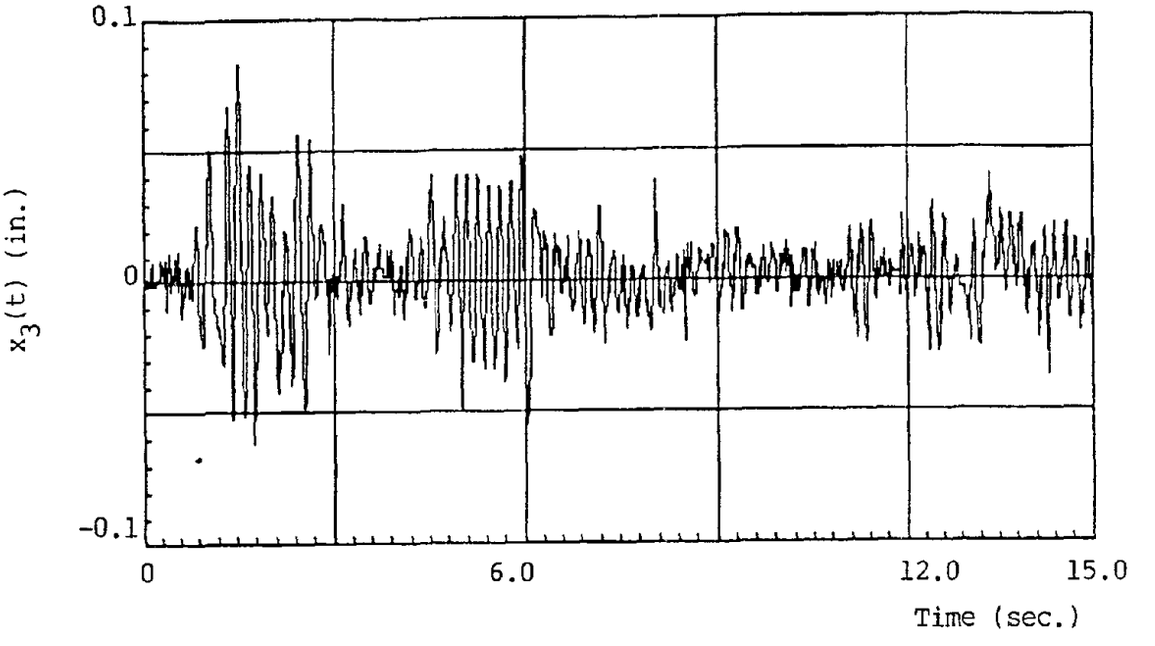

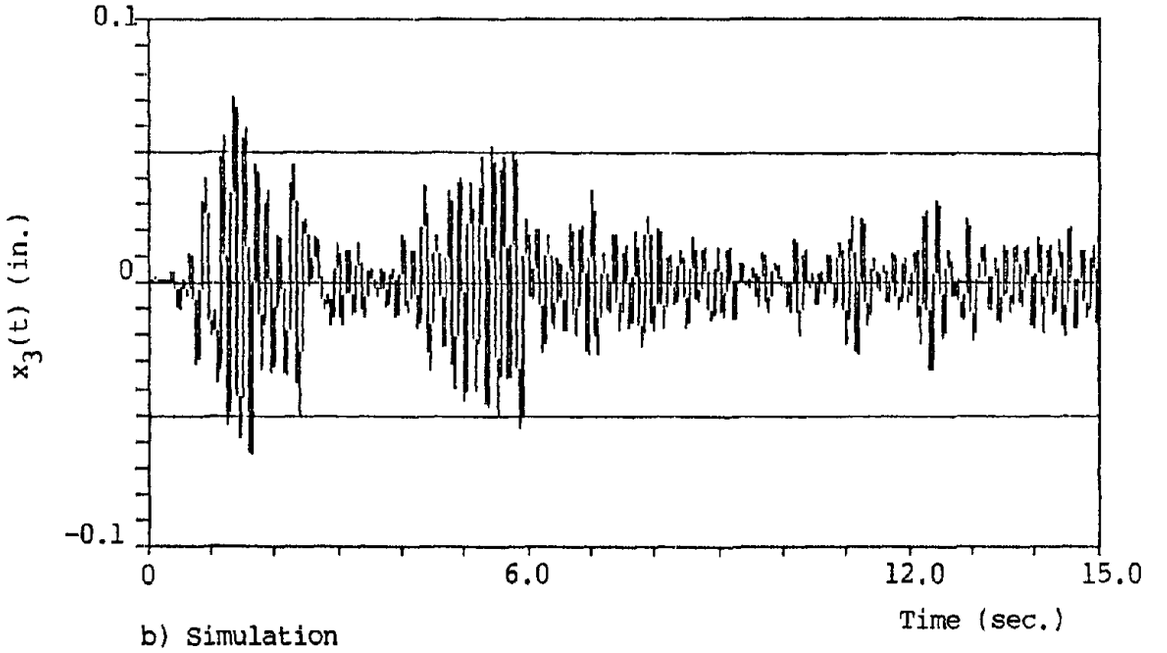

b) Simulation

FIG. 4.13. Third-floor Relative Displacement for Case 1 ($T = 22.2^{\circ}C$)

simulation, some discrepancy exists in the absolute acceleration values computed in the simulation. This can be seen by comparing Tables 4.1 and 4.3.

A comparison of the results produced by the three different damper configurations reveals, as expected, that case 1, with dampers added to all floors, is the optimal one for reducing structural response. However, the experimental and simulated results suggest that the effectiveness of VE dampers is governed more by their placements within the structure than by their sheer number. The problem of optimum placement of VE dampers is one of significant importance and needs to be explored further.

Based on the experimental and simulated results, it can be readily seen that the addition of VE dampers is effective in reducing structural response due to seismic excitation. Also, its effectiveness increases as the temperature increases.

CASE	CONFIGURATION OF STRUCTURE	RESPONSES	FLOOR	NO DAMPERS (REFERENCE)	WITH DAMPERS			
					AMBIENT TEMPERA.		HIGHER TEMPERA.	
				MAX. VAL.	MAX.VAL.	RED. %	MAX.VAL.	RED. %
1	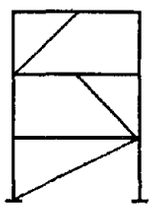	Relative Displacement (in)	1	0.1675	0.0326	80.5	0.0329	80.4
			2	0.2642	0.0525	80.1	0.0482	81.8
			3	0.3560	0.0830	76.7	0.0691	80.6
		Storydrift Displacement (in)	0-1	0.1675	0.0326	80.5	0.0329	80.4
			1-2	0.1367	0.0416	69.6	0.0495	63.8
			2-3	0.1172	0.0427	63.6	0.0494	57.8
		Absolute Acceleration (g's)	1	0.2345	0.1170	50.3	0.0961	61.1
			2	0.2588	0.1784	31.1	0.1213	53.1
			3	0.3484	0.2373	31.9	0.1862	46.6
2	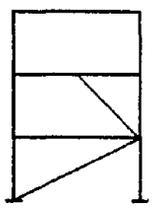	Relative Displacement (in)	1	0.3159	0.0378	88.0	0.0325	89.7
			2	0.4180	0.0775	81.5	0.0723	82.7
			3	0.5181	0.2102	59.4	0.1419	72.6
		Storydrift Displacement (in)	0-1	0.3159	0.0378	88.0	0.0325	89.7
			1-2	0.1547	0.0615	60.2	0.0623	59.7
			2-3	0.1910	0.1377	27.9	0.0979	48.7
		Absolute Acceleration (g's)	1	0.3623	0.1073	70.4	0.1081	70.2
			2	0.3233	0.1923	40.5	0.1483	54.1
			3	0.4840	0.4134	14.6	0.2766	42.8
3	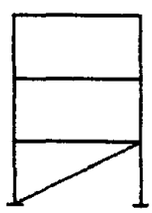	Relative Displacement (in)	1	0.3234	0.0511	84.2	0.0467	85.6
			2	0.4963	0.2865	42.3	0.1745	64.8
			3	0.5935	0.4521	23.8	0.2864	52.0
		Storydrift Displacement (in)	0-1	0.3234	0.0511	84.2	0.0467	85.6
			1-2	0.1924	0.2448	-19.2	0.1365	29.1
			2-3	0.1821	0.2054	-12.8	0.1277	29.9
		Absolute Acceleration (g's)	1	0.2889	0.1058	63.4	0.0945	67.3
			2	0.2242	0.2916	-30.1	0.1968	12.2
			3	0.3769	0.3711	1.5	0.2688	28.7

TABLE 4.1. Experimental Results - MDOF System and Seismic Input

CASE	CONFIGURATION OF STRUCTURE	PARAMETERS	MODE	NO DAMPERS (REFERENCE)	WITH DAMPERS	
					AMBIENT TEMPERATURE	HIGHER TEMPERATURE
1	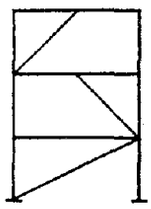	Natural Frequency (Hz)	1	2.54	5.76	5.18
			2	7.71	14.84	14.36
			3	12.99	19.04	18.85
		Damping Factor (%)	1	1.684	2.052	12.935
			2	0.621	2.679	5.956
			3	0.155	4.996	4.026
2	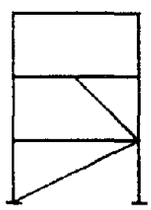	Natural Frequency (Hz)	1	2.05	4.30	3.91
			2	5.96	11.04	10.55
			3	12.04	19.24	18.85
		Damping Factor (%)	1	2.523	3.10	11.0
			2	0.28	3.52	5.81
			3	0.075	6.45	5.47
3	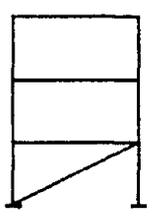	Natural Frequency (Hz)	1	1.855	2.734	2.734
			2	6.25	9.765	9.668
			3	11.23	18.85	17.875
		Damping Factor (%)	1	2.566	1.482	2.78
			2	1.025	0.892	2.51
			3	0.164	2.566	7.54

TABLE 4.2. System Parameters Based on Experimental Results

CASE	CONFIGURATION OF STRUCTURE	RESPONSES	FLOOR	NO DAMPERS (REFERENCE)	WITH DAMPERS			
					AMBIENT TEMPERA.		HIGHER TEMPERA.	
				MAX. VAL.	MAX.VAL.	RED. %	MAX.VAL.	RED. %
1	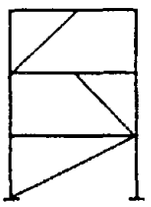	Relative Displacement (in)	1	0.1339	0.0158	88.2	0.0146	89.1
			2	0.2176	0.0462	78.8	0.0351	83.9
			3	0.2758	0.0703	74.5	0.0507	81.6
		Storydrift Displacement (in)	0-1	0.1339	0.0158	88.2	0.0146	89.1
			1-2	0.0932	0.0304	67.4	0.0205	78.0
			2-3	0.0688	0.0279	56.8	0.0183	73.4
		Absolute Acceleration (g's)	1	0.1804	0.1202	33.4	0.1009	44.1
			2	0.1629	0.2292	-40.6	0.1323	18.8
			3	0.2496	0.2692	-7.8	0.1722	31.0
2	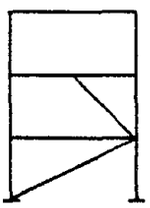	Relative Displacement (in)	1	0.2644	0.0262	90.0	0.0323	87.8
			2	0.3769	0.0701	81.4	0.0666	82.3
			3	0.4721	0.1815	61.6	0.1358	71.2
		Storydrift Displacement (in)	0-1	0.2644	0.0262	90.0	0.0323	87.8
			1-2	0.1125	0.0439	61.0	0.0346	69.2
			2-3	0.0953	0.1149	-20.6	0.0733	23.1
		Absolute Acceleration (g's)	1	0.1205	0.1156	4.1	0.1088	9.7
			2	0.1606	0.2076	-29.3	0.1472	11.5
			3	0.2283	0.3383	-48.2	0.2337	-2.4
3	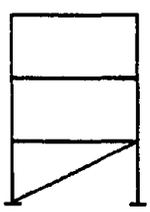	Relative Displacement (in)	1	0.2336	0.0210	91.0	0.0244	89.6
			2	0.3572	0.1672	53.2	0.1505	57.9
			3	0.5129	0.2737	46.6	0.2586	49.6
		Storydrift Displacement (in)	0-1	0.2336	0.0210	91.0	0.0244	89.6
			1-2	0.1356	0.1466	-8.1	0.1272	6.2
			2-3	0.1623	0.1168	28.0	0.1173	27.7
		Absolute Acceleration (g's)	1	0.1627	0.1396	14.2	0.1108	31.9
			2	0.1443	0.2140	-48.3	0.1900	-31.7
			3	0.2568	0.2280	11.2	0.2165	15.7

TABLE 4.3. Simulation Results

SECTION 5

CONCLUDING REMARKS

An experimental investigation was conducted to determine whether viscoelastic dampers, when installed in a building structure, can be effective in reducing structural response to seismic excitations. The experiments were performed using a 1:4 scale model structure simulating a multi-degree-of-freedom frame structure whose base motion was supplied by a shaking table. By proper bracing, a single-degree-of-freedom as well as a multi-degree-of-freedom system was simulated.

Experimental as well as simulation results show that significant improvement of structural performance under seismic conditions can be realized with addition of VE dampers at appropriate locations. In the single-degree-of-freedom case, it was shown that reductions in response can be as high as 87% for the relative displacement and 60% for the absolute acceleration. Results for the multi-degree-of-freedom case show that, with the most favorable damper configuration, the average reductions in structural response were 80% for relative displacements 70% for storydrifts and about 50% for absolute accelerations.

Comparisons were made between the experimental and simulation results. These comparisons show good agreement, suggesting that the basic assumptions made in the theoretical considerations are valid. And the simulation procedure developed in this study can be used for extrapolation of results to other cases of interest.

Temperature dependency of the VE dampers was carefully studied in this investigation. The experiments were carried out at temperatures ranging from 22°C to 35°C and the results show that the damper properties and their efficiency are strongly temperature dependent. Hence, environmental temperature must be taken into account when designing dampers for

structural applications.

Attention was also paid to damper configurations. Diagonal placement of the dampers was the best in case of the SDOF system since the relative displacement is the greatest in this position and so is the energy dissipated by the damper. Similar considerations were given to experiments involving multi-degree-of-freedom systems and the advantage of optimum damper placement was also clearly demonstrated.

One limitation associated with this experimental investigation has to do with the fact that, since the model structure is light in comparison with the weight of dampers and their fixtures, the addition of dampers not only resulted in an increase in its damping ratio, but also its stiffness. A significant increase in stiffness is generally not expected in real structural applications and hence the results presented in this study must be interpreted with care. However, simulation studies have been made under the assumption of no increase in stiffness which support the general conclusions stated above.

Finally, while damper additions are accompanied by damping increases in the structure, their effectiveness in structural response reduction diminishes as damping is increased beyond a certain range. In this connection, results in relative displacement and absolute acceleration for the SDOF system were generated through simulation as functions of the damping ratio while the structural stiffness or natural frequency was kept constant (5.124 HZ). These are shown in Figs. 5.1 and 5.2 which demonstrate this diminishing effect when the damping ratio is increased beyond 0.2.

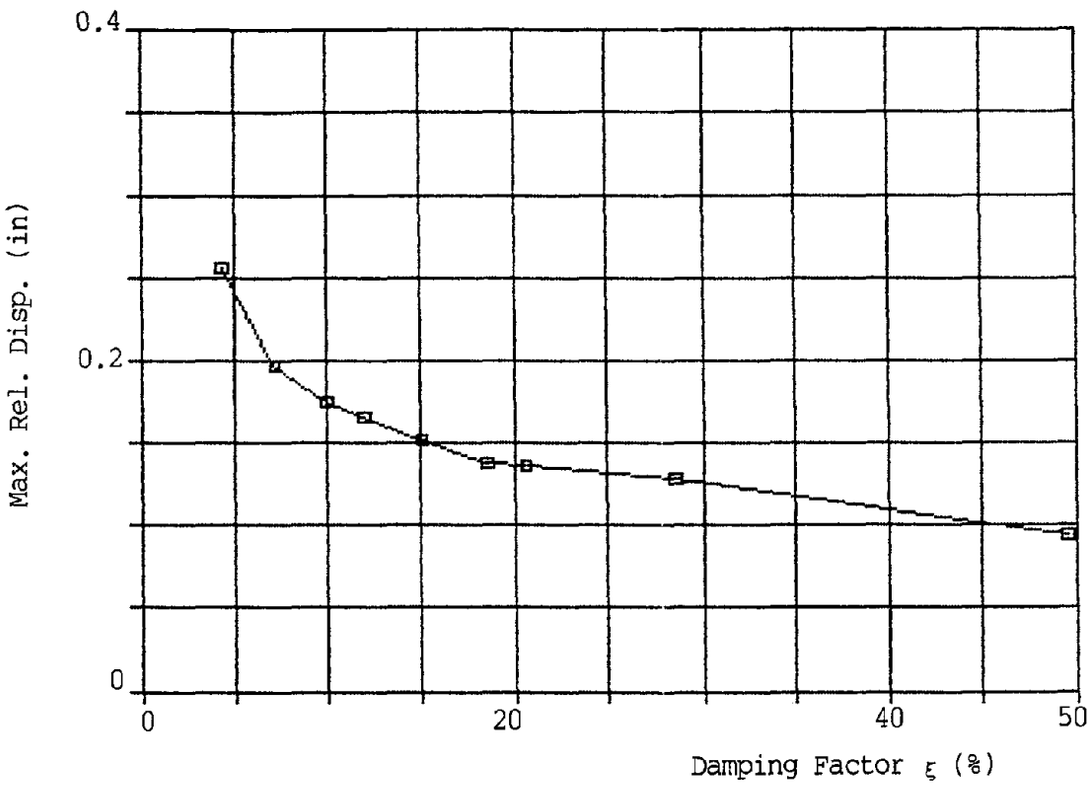

FIG. 5.1. Maximum Relative Displacement as a Function of Damping Ratio

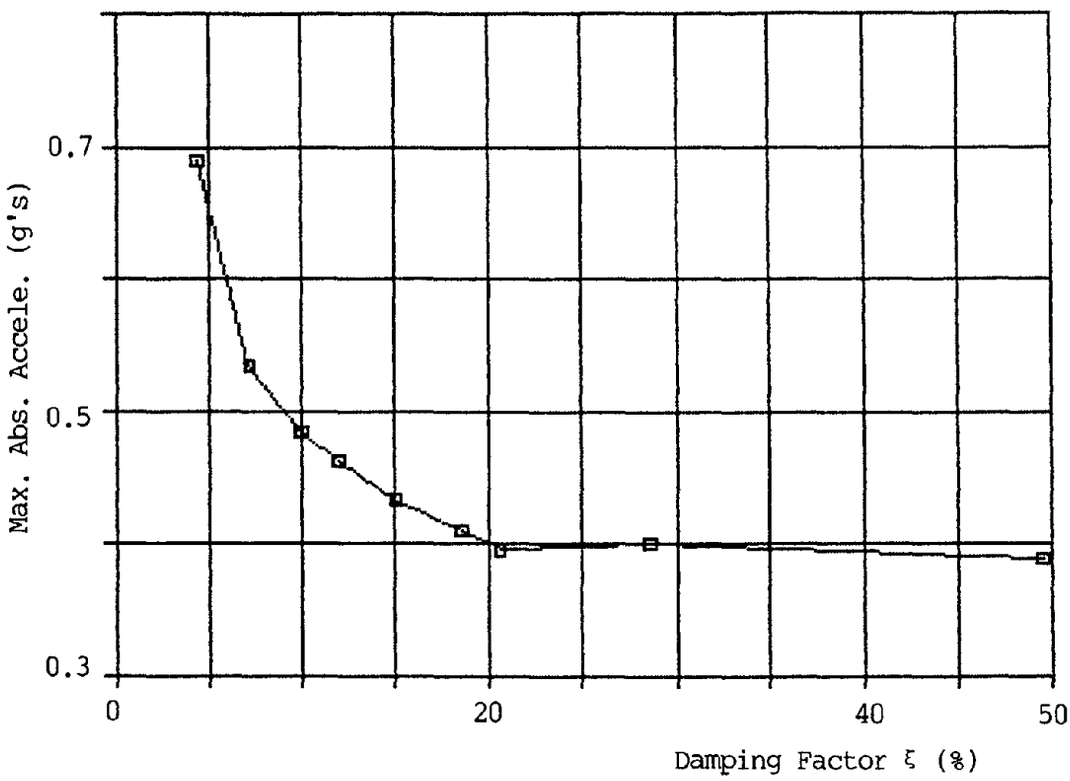

FIG. 5.2. Maximum Absolute Acceleration as a Function of Damping Ratio

REFERENCES

1. P. Mahmoodi, 'Design and Analysis of Viscoelastic Vibration Dampers for Structures,' Proc. INOVA-73 World Innovative Week Conference, E.D. Eyrolles, Paris, 25-39 (1974).

2. P. Mahmoodi, 'Structural Dampers,' J. Struct. Div., ASCE, 95, ST8, 1661-1672 (1972).

3. C.J. Keel and P. Mahmoodi, 'Designing of Viscoelastic Dampers for Columbia Center Building,' in Building Motion in Wind, N. Isyumov and T. Tschanz (eds.), ASCE, New York, 66-82 (1986).

4. P. Mahmoodi and C.J. Keel, 'Performance of Structural Dampers for the Columbia Center Building,' in Building Motion in Wind, ASCE, New York, 83-106 (1986).

5. R.H. Zhang, T.T. Soong and P. Mahmoodi, 'Seismic Response of Steel Frame Structures with Added Viscoelastic Dampers,' J. Earthquake Engineering and Structural Dynamics, submitted.

6. T.T. Soong, A.M. Reinhorn and J.N. Yang, 'A Standardized Model for Structural Control Experiments and Some Experimental Results,' in Active Control, H.H.E. Leipholz (ed.), Martinus Nijhoff Pub., 669-693 (1987).

7. R.W. Clough and J. Penzien, Dynamics of Structures, McGraw-Hill, New York (1975).

NATIONAL CENTER FOR EARTHQUAKE ENGINEERING RESEARCH
LIST OF PUBLISHED TECHNICAL REPORTS

The National Center for Earthquake Engineering Research (NCEER) publishes technical reports on a variety of subjects related to earthquake engineering written by authors funded through NCEER. These reports are available from both NCEER's Publications Department and the National Technical Information Service (NTIS). Requests for reports should be directed to the Publications Department, National Center for Earthquake Engineering Research, State University of New York at Buffalo, Red Jacket Quadrangle, Buffalo, New York 14261. Reports can also be requested through NTIS, 5285 Port Royal Road, Springfield, Virginia 22161. NTIS accession numbers are shown in parenthesis, if available.

NCEER-87-0001 "First-Year Program in Research, Education and Technology Transfer," 3/5/87, (PB88-134275/AS).

NCEER-87-0002 "Experimental Evaluation of Instantaneous Optimal Algorithms for Structural Control," by R.C. Lin, T.T. Soong and A.M. Reinhorn, 4/20/87, (PB88-134341/AS).

NCEER-87-0003 "Experimentation Using the Earthquake Simulation Facilities at University at Buffalo," by A.M. Reinhorn and R.L. Ketter, to be published.

NCEER-87-0004 "The System Characteristics and Performance of a Shaking Table," by J.S. Hwang, K.C. Chang and G.C. Lee, 6/1/87, (PB88-134259/AS).

NCEER-87-0005 "A Finite Element Formulation for Nonlinear Viscoplastic Material Using a Q Model," by O. Gyebi and G. Dasgupta, 11/2/87, (PB88-213764/AS).

NCEER-87-0006 "Symbolic Manipulation Program (SMP) - Algebraic Codes for Two and Three Dimensional Finite Element Formulations," by X. Lee and G. Dasgupta, 11/9/87, (PB88-219522/AS).

NCEER-87-0007 "Instantaneous Optimal Control Laws for Tall Buildings Under Seismic Excitations," by J.N. Yang, A. Akbarpour and P. Ghaemmaghami, 6/10/87, (PB88-134333/AS).

NCEER-87-0008 "IDARC: Inelastic Damage Analysis of Reinforced Concrete-Frame Shear-Wall Structures," by Y.J. Park, A.M. Reinhorn and S.K. Kunnath, 7/20/87, (PB88-134325/AS).

NCEER-87-0009 "Liquefaction Potential for New York State: A Preliminary Report on Sites in Manhattan and Buffalo," by M. Budhu, V. Vijayakumar, R.F. Giese and L. Baumgras, 8/31/87, (PB88-163704/AS).

NCEER-87-0010 "Vertical and Torsional Vibration of Foundations in Inhomogeneous Media," by A.S. Veletsos and K.W. Dotson, 6/1/87, (PB88-134291/AS).

NCEER-87-0011 "Seismic Probabilistic Risk Assessment and Seismic Margin Studies for Nuclear Power Plants," by Howard H.M. Hwang, 6/15/87, (PB88-134267/AS).

NCEER-87-0012 "Parametric Studies of Frequency Response of Secondary Systems Under Ground-Acceleration Excitations," by Y. Yong and Y.K. Lin, 6/10/87, (PB88-134309/AS).

NCEER-87-0013 "Frequency Response of Secondary Systems Under Seismic Excitations," by J.A. HoLung, J. Cai and Y.K. Lin, 7/31/87, (PB88-134317/AS).

NCEER-87-0014 "Modelling Earthquake Ground Motions in Seismically Active Regions Using Parametric Time Series Methods," G.W. Ellis and A.S. Cakmak, 8/25/87, (PB88-134283/AS).

NCEER-87-0015 "Detection and Assessment of Seismic Structural Damage," by E. DiPasquale and A.S. Cakmak, 8/25/87, (PB88-163712/AS).

NCEER-87-0016 "Pipeline Experiment at Parkfield, California," by J. Isenberg and E. Richardson, 9/15/87, (PB88-163720/AS).

NCEER-87-0017 "Digital Simulations of Seismic Ground Motion," by M. Shinozuka, G. Deodatis and T. Harada, 8/31/87, (PB88-155197/AS).

NCEER-87-0018 "Practical Considerations for Structural Control: System Uncertainty, System Time Delay and Truncation of Small Forces," J. Yang and A. Akbarpour, 8/10/87, (PB88-163738/AS).

NCEER-87-0019 "Modal Analysis of Nonclassically Damped Structural Systems Using Canonical Transformation," by J.N. Yang, S. Sarkani and F.X. Long, 9/27/87, (PB88-187851/AS).

NCEER-87-0020 "A Nonstationary Solution in Random Vibration Theory," by J.R. Red-Horse and P.D. Spanos, 11/3/87, (PB88-163746/AS).

NCEER-87-0021 "Horizontal Impedances for Radially Inhomogeneous Viscoelastic Soil Layers," by A.S. Veletsos and K.W. Dotson, 10/15/87, (PB88-150859/AS).

NCEER-87-0022 "Seismic Damage Assessment of Reinforced Concrete Members," by Y.S. Chung, C. Meyer and M. Shinozuka, 10/9/87, (PB88-150867/AS).

NCEER-87-0023 "Active Structural Control in Civil Engineering," by T.T. Soong, 11/11/87, (PB88-187778/AS).

NCEER-87-0024 "Vertical and Torsional Impedances for Radially Inhomogeneous Viscoelastic Soil Layers," by K.W. Dotson and A.S. Veletsos, 12/87, (PB88-187786/AS).

NCEER-87-0025 "Proceedings from the Symposium on Seismic Hazards, Ground Motions, Soil-Liquefaction and Engineering Practice in Eastern North America, October 20-22, 1987, edited by K.H. Jacob, 12/87, (PB88-188115/AS).

NCEER-87-0026 "Report on the Whittier-Narrows, California, Earthquake of October 1, 1987," by J. Pantelic and A. Reinhorn, 11/87, (PB88-187752/AS).

NCEER-87-0027 "Design of a Modular Program for Transient Nonlinear Analysis of Large 3-D Building Structures," by S. Srivastav and J.F. Abel, 12/30/87, (PB88-187950/AS).

NCEER-87-0028 "Second-Year Program in Research, Education and Technology Transfer," 3/8/88, (PB88-219480/AS).

NCEER-88-0001 "Workshop on Seismic Computer Analysis and Design With Interactive Graphics," by J.F. Abel and C.H. Conley, 1/18/88, (PB88-187760/AS).

NCEER-88-0002 "Optimal Control of Nonlinear Structures," J.N. Yang, F.X. Long and D. Wong, 1/22/88, (PB88-213772/AS).

NCEER-88-0003 "Substructuring Techniques in the Time Domain for Primary-Secondary Structural Systems," by G. D. Manolis and G. Juhn, 2/10/88, (PB88-213780/AS).

NCEER-88-0004 "Iterative Seismic Analysis of Primary-Secondary Systems," by A. Singhal, L.D. Lutes and P. Spanos, 2/23/88, (PB88-213798/AS).

NCEER-88-0005 "Stochastic Finite Element Expansion for Random Media," P. D. Spanos and R. Ghanem, 3/14/88, (PB88-213806/AS).

NCEER-88-0006 "Combining Structural Optimization and Structural Control," F. Y. Cheng and C. P. Pantelides, 1/10/88, (PB88-213814/AS).

NCEER-88-0007 "Seismic Performance Assessment of Code-Designed Structures," H.H-M. Hwang, J. Jaw and H. Shau, 3/20/88, (PB88-219423/AS).

NCEER-88-0008 "Reliability Analysis of Code-Designed Structures Under Natural Hazards," H.H-M. Hwang, H. Ushiba and M. Shinozuka, 2/29/88.

NCEER-88-0009 "Seismic Fragility Analysis of Shear Wall Structures," J-W Jaw and H.H-M. Hwang, 4/30/88.

NCEER-88-0010 "Base Isolation of a Multi-Story Building Under a Harmonic Ground Motion - A Comparison of Performances of Various Systems," F-G Fan, G. Ahmadi and I.G. Tadjbakhsh, to be published.

NCEER-88-0011 "Seismic Floor Response Spectra for a Combined System by Green's Functions," F.M. Lavelle, L.A. Bergman and P.D. Spanos, 5/1/88.

NCEER-88-0012 "A New Solution Technique for Randomly Excited Hysteretic Structures," G.Q. Cai and Y.K. Lin, 5/16/88.

NCEER-88-0013 "A Study of Radiation Damping and Soil-Structure Interaction Effects in the Centrifuge," K. Weissman, supervised by J.H. Prevost, 5/24/88, to be published.

NCEER-88-0014 "Parameter Identification and Implementation of a Kinematic Plasticity Model for Frictional Soils," J.H. Prevost and D.V. Griffiths, to be published.

NCEER-88-0015 "Two- and Three-Dimensional Dynamic Finite Element Analyses of the Long Valley Dam," D.V. Griffiths and J.H. Prevost, to be published.

NCEER-88-0016 "Damage Assessment of Reinforced Concrete Structures in Eastern United States," A.M. Reinhorn, M.J. Seidel, S.K. Kunnath and Y.J. Park, 6/15/88.

NCEER-88-0017 "Dynamic Compliance of Vertically Loaded Strip Foundations in Multilayered Viscoelastic Soils," S. Ahmad and A.S.M. Israil, 6/17/88.

NCEER-88-0018 "An Experimental Study of Seismic Structural Response With Added Viscoelastic Dampers," R.C. Lin, Z. Liang, T.T. Soong and R.H. Zhang, 6/30/88.